Design and Testing of an Amphibious AUV

A Major Qualifying Project

Submitted to the Faculty of

WORCESTER POLYTECHNIC INSTITUTE

in Partial Fulfillment of the Requirements for the

Degree of Bachelor of Science in

Aerospace Engineering

by

Ryan Chesanek

Graham Driscoll-Carignan

Spencer Granlund

Matthew McMahon

Evan Russell

Benjamin Twombly

MARCH 1, 2024

Approved by:
Professor Michael A. Demetriou,
Worcester Polytechnic Institute

Abstract

The goal of this project is to design, assemble, and test an autonomous underwater vehicle (AUV) that can seamlessly transition between aerial flight and underwater movement. The system comprises a quadrotor structure equipped with a waterproof enclosure containing the necessary electronics and microcontroller to enable autonomous flight. All these operations are carried out autonomously through a Pixhawk flight controller that incorporates a Raspberry Pi companion computer and a comprehensive sensor array. To showcase these capabilities, the designed quadrotor is tasked with completing a mission in an indoor swimming pool. The AUV begins on the poolside, takes off vertically, hovers stably above the water's surface, lands on the water, submerges three feet, and covers 20 feet underwater, resurfaces, and then returns to its starting position. This paper outlines the design process and the iterative steps taken, as well as the research undertaken to improve and enhance each iteration.

Acknowledgments

The team maintained a regular weekly meeting schedule with Professor Demetriou to discuss progress. At the start of the project, the group met with Michael Beskid and Toshak Patel, previous MQP team members, to gain insights into best practices and lessons learned. Furthermore, the team had the privilege of meeting with Randy Holtgrefe to delve into discussions regarding component selection. All authors extend their gratitude to Professor Michael Demetriou, Michael Beskid, Toshak Patel, and Randy Holtgrefe for their support and guidance throughout the project's duration.

Table of Authorship

Introduction	
Overview	Evan Russell
Project Objectives	Ben Twombly and Evan Russell
Design Requirements, Constrains, and Considerations	Matthew McMahon
Project Management and Team Organization	Matthew McMahon
Budget Overview and Analysis	Matthew McMahon
Societal Impacts	Spencer Granlund
Background	
Brief History	Graham Driscoll-Carignan
Literature Review	Graham Driscoll-Carignan
Coordinate Systems	Evan Russell
Quadcopter Flight Mechanics	Evan Russell
Equations of Motion	Evan Russell
Aerial Dynamics	Evan Russell
Aerial Dynamics - Validation	Evan Russell
Aerial Dynamics - Analysis	Evan Russell
Quadplane Flight Mechanics	Evan Russell
Underwater Dynamics	Evan Russell
Technical Selections	
Flight Controller	Spencer Granlund
Companion Computer	Spencer Granlund
Power Subsystem	Spencer Granlund
Propulsion Subsystem	Spencer Granlund
Sensing and Localization Subsystem	Spencer Granlund
Ardupilot & Frame Type	Spencer Granlund
MAVLink	Spencer Granlund
Autonomy Scripts	Spencer Granlund
Control Architecture	Graham Driscoll-Carignan
Quadrotor Frame Design	Ryan Chesanek
Enclosure and Flight Hardware Positioning	Ryan Chesanek
Material Selection	Ryan Chesanek
Electronic Enclosure	Ryan Chesanek
Camera Enclosure	Ryan Chesanek
Tilt Rotor Design	Ryan Chesanek
Waterproof Servo	Ryan Chesanek
Hydrostatics Analysis	Evan Russell
Propeller Choice	Ben Twombly
Aerial and Underwater Efficiency Analysis	Ben Twombly

Results	
Summary	Ben Twombly and Spencer Granlund
Conclusions	Ben Twombly
Recommendations for Future Work	Ryan Chesanek and Spencer Granlund
Broader Impact	Graham Driscoll-Carignan

Table of Contents

List of Figures

List of Tables

1 Introduction

1.1 Overview

Autonomous Underwater Vehicles (AUVs) with the capability of both aerial flight and underwater locomotion are a groundbreaking advancement in marine technology. The technological advancement of these hybrid vehicles has been marked by interdisciplinary collaboration, combining expertise in aerospace, robotics, and marine engineering. The integration of aerial flight capabilities enhances the versatility of AUVs, allowing them to survey vast oceanic expanses more efficiently and rapidly than traditional underwater vehicles. This development has significant implications for various applications, ranging from marine research and environmental monitoring to defense and commercial industries. This high-tech emergence not only expands our understanding of the ocean but also presents innovative solutions to address challenges across various domains, leading to a new era of marine technology.

1.2 Project Objectives

This project's objective was to design, build, and test an AUV for combined aerial and aquatic navigation. The mission design requirements were as follows: first, for the AUV to perform a vertical takeoff and move above the pool water surface. Then, the AUV will descend onto the water and submerge itself to a depth of three feet. Next, the quadrotor must travel at this depth for twenty feet before resurfacing and returning to its takeoff location. Figure 1 depicts the autonomous flight path of the AUV, with each stage numbered in succession.

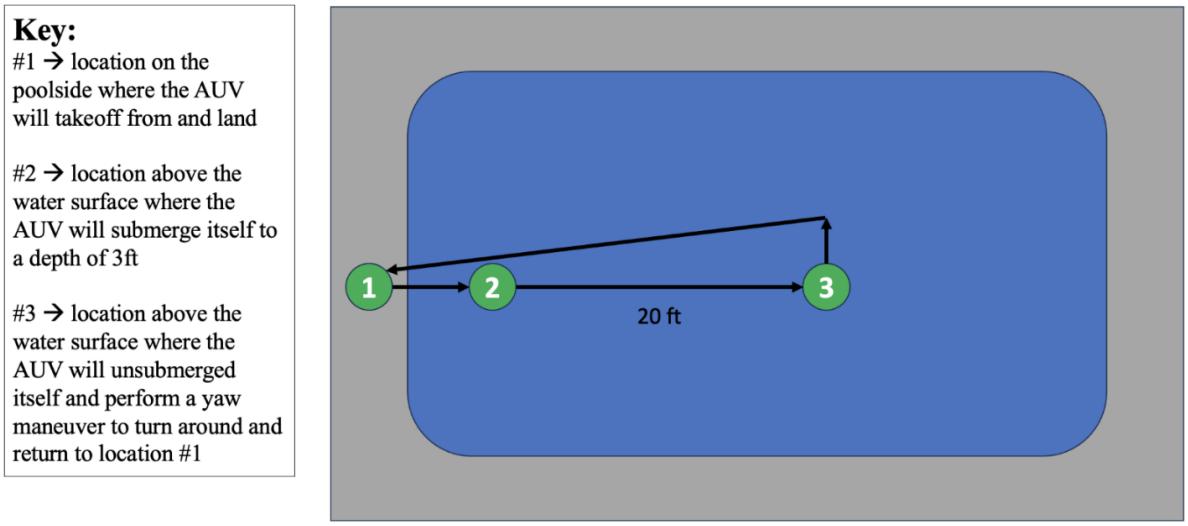

Figure 1: Schematic of AUV's autonomous flight path.

The design's main requirement was for the AUV to be capable of aerial and aquatic maneuverability. One stipulation of the project was the AUV must be capable of transitioning between aerial and underwater operation “at-will”, eliminating the need for separate setups for

each mode and ensuring readiness for either without additional modifications. The control of the AUV had to be fully autonomous and must be capable of navigating in a GPS-denied environment. These requirements and constraints forced a unique set of factors to be considered in the design.

Firstly, the need for a propulsion system capable of being utilized in both environments was one of the considerations that influenced the entire design process. In aerial flight, it needed to output thrust greater than the vehicle's weight for the entire flight duration. This meant that the propulsion system needed to be highly efficient in air, while also being able to operate and maintain some degree of efficiency underwater. This was difficult due to the differing properties of the two fluids.

Both the vehicle's weight and buoyancy were another design consideration. Weight was a concern primarily for aerial flight, with the need for the propulsion to be capable of a thrust-to-weight ratio greater than one for an extended period. This required component weight to be a factor in the design process, and influenced what systems and hardware were incorporated into the design. Buoyancy of the vehicle was also important, as sufficient positive or negative buoyancy would greatly increase the strain passively placed upon the propulsion while underwater. For this reason, the goal was to get the quadrotor as close to neutral buoyancy as possible.

Static stability in both the air and underwater environments had to also be considered. Both the location of the center-of-mass and center-of-buoyancy of the AUV had to be known, meaning that the focus was not only on the distribution of weight but also on the density of different parts of the AUV’s structure. This was made particularly complex due to the need for a watertight enclosure for the flight hardware and electronics.

Waterproofing of the various components and electronics was another major consideration, with the need for sustained underwater operation necessitating the need for a watertight enclosure. This aspect was one of the greatest difficulties for the previous MQP group, with continuous problems with leaks stemming from various design decisions. Considerations also had to be made for the ease of access to the components inside said enclosure, to ensure ability to make modifications and allow for testing.

While the aerial flight dynamics of a quadrotor are well documented and studied due to their extreme prevalence among commercially available and homemade quadrotors, the same cannot be said for quadrotors in an underwater environment. Much of the previous MQP group’s research centered around this issue, however their AUV utilized a ballast system to alter the static stability to control the orientation of the AUV in the water. This ballast system caused significant difficulties for them, so our team decided to pursue the approach of using a gimbaled front axis to change the orientation of the propulsion system rather than rotating the entire vehicle 90 degrees. This is similar to a quadplane setup but not the exact same. This means the team had to explore and derive the dynamics of this kind of vehicle and how it was affected by various hydrostatic and hydrodynamic forces.

Lastly, the consideration of navigation both in the air and underwater autonomously in a GPS-denied area had to be considered. Most examples of fully autonomous navigation in commercially available quadrotors utilized GPS for this purpose. Therefore, the AUV had to establish its own inertial frame and localize its position with onboard IMUs and a camera.

1.3 Design Requirements, Constraints, and Considerations

The Goal of this project is to design, manufacture, and test a quadrotor AUV that meets the following design requirements:

- Stable, Autonomous, GPS denied aerial flight
- Aerial autonomous navigation between predetermined locations
- Transition from air to water transition from water to air
- Stable, Autonomous, GPS denied aquatic flight.
- Aquatic autonomous navigation between predetermined locations
- Combined, at will autonomous aerial and aquatic flight

There are various key constraints that hinder the success of this project. Time is the biggest limitation of this project is that it is to be completed within the timespan of August 2023 until March 2024. This is the duration of WPI's A, B, and C terms of the 2023-24 academic calendar. In addition, the budget for this project is $250 per team member, for a total of $1500. We would also like to acknowledge the following considerations:

- Adherence to FAA (Federal Aviation Administration) regulations regarding quadrotors, particularly in Parks and Recreational spaces
- Adherence to WPI rules and regulations.
- Adherence for WPI Sports & Recreation Center policy and Pool Regulations. Namely, we want to ensure that WPI's pool is not contaminated with any substances or debris.
- We would also like to acknowledge the safety risks involved with the use of highspeed propellers, batteries, and low voltage electricity in the WPI swimming pool.

1.4 Project Management and Team Organization

The project team consists of a six-member team accompanied by an advising Professor from the Aerospace Engineering Department. The members Ryan Chesanek, Graham Driscoll-Carignan, Spencer Granlund, Matthew McMahon, Evan Russell, and Benjamin Twombly were advised by Professor Demetriou. The team met with Professor Demetriou once a week to present their weekly progress. This weekly meeting shifted for each term but remained on Wednesdays and Thursdays. Additionally, the whole student team met on two occasions every week, on Tuesdays and Fridays from 2pm to 5pm.

The initial division of responsibilities consisted of loose organization into three sub-teams dealing with the propulsion, structures, and navigation & controls. Assignment of group members to said sub-teams was done first based on prior experience and familiarity with aspects of the project, such as prior knowledge of quadrotor flight-control systems and software. While not final or absolute, this provided a preliminary framework for group members to focus their efforts. The Propulsion team was comprised of Matt and Evan. Their main objectives were to design the propeller and motor subsystem. They calculated the aerial and aquatic dynamics of the quadrotor and completed hydrostatic and hydrodynamic analysis. The Structures team was comprised of Ryan and Graham, whose main objective was to design the framework for the quadrotor. They designed the framework for the waterproof enclosure, rotor arms, and the gimballing of the front to rotors on a single axis. The Controls and Navigation team was comprised of Spencer and Ben. This sub-team developed all the electronics and wiring that allowed the quadrotor to fly. They designed the autonomy scripts and implemented the ArduPilot and ArduCopter software. This initial division of responsibilities began to mesh because there is a significant overlap between the given roles. Each subsystem has a large influence on all the

other subsystems. Towards the project's later stages, variations were laid out, such as members focusing on conference and report preparation, or creating models and visuals for the final presentation.

1.5 Budget Overview and Analysis

The total budget afforded for this project was $1500 as determined by the standard university policy of $250 per group member. It was one of the primary considerations in much of the general design and decision-making in the initial planning and research stages. The limited budget presented many restrictions on how certain portions of the project could be approached. Some components were reused from the previous year's iteration of the project, and others were already available either in the laboratory or elsewhere. Specifically, the T265 tracking camera had been purchased by the previous year's group and thus was already available. Second the Pixhawk flight controller was available in the laboratory. Lastly, many of the structural components were 3D-printed, the printers utilized for this were already available to group members. All other components and hardware were purchased from a variety of vendors, the breakdown of the budget usage for these components is shown in Table 1. In the table below, a full list of purchases is described with hyperlinks to the product, the units purchased, and the unit price. The red highlights indicate that the purchase was not used in our project and is not recommended. It is our hope that many of the purchases that we have made will support the design of future iterations of this project.

$1500 Budget Breakdown			
Supplier	**Product**	**Quantity**	**Unit Price**
Amazon	4 in 1 Electronic Speed Controller	1	$55.90
Amazon	Pixhawk Power Module	1	$9.99
Amazon	DC-DC Converter Step Down UBEC Module	2	$7.98
Amazon	M to F Connectors with Battery Connector Adapter	1	$7.99
Amazon	Female Plugs RC Battery Charger Adapter	1	$8.99
Amazon	100pcs 3D Printing Brass Nuts	1	$8.59
Amazon	2pcs Amass XT60 M to XT60 FM	1	$10.50
Amazon	14 Gauge 3 Conductor Electrical Wire	1	$21.88
Amazon	1 Foot plastic, Clear acrylic PVC pipe	1	$21.99
Amazon	USB Extension Cable 1 ft	1	$6.50
Amazon	3M Marine Adhesive Sealant	2	$17.68
Amazon	20Pair Gold Bullet Banana Plug	1	$7.80
Amazon	7035 Reinforced Glass Fiber Nylon Propellers 7in	1	$18.98
Amazon	INJORA 7KG 2065 Digital Servo	6	~$16.50
Amazon	INJORA 25T Servo Arm	2	$8.99
Amazon	Tenergy TB-6AB Balance Charger	1	$35.99
Amazon	Anycubic ABS-Like + 3D Printer Resin	1	$27.99
HomeDepot	3 in. Heavy Duty Flexible Rubber Cap	1	$9.08
HomeDepot	3 in. PVC DWV Cap	1	$9.87
HomeDepot	8 oz. Regular Clear PVC Cement	1	$7.96

Get FPV	T-Motor VELOX V2812 Cinematic Motor - 925KV	4	$33.99
Grainger	Carbon Fiber Rod: 1/2 in Overall Dia	2	$33.78
Amazon	Radiolink R9DS 2.4GHz RC Receiver	1	$21.99
Amazon	400 Pcs Wire Heat Shrink Tubing Kit	1	$7.99
Amazon	5 Pcs Polycarbonate Sheets	1	$9.99
Amazon	Adhesive Hook and Loop Style Sheets	1	$9.99
Amazon	Bondo Fiberglass Resin	1	$31.98
Amazon	AAFB Electrical Tape Pack	1	$6.49
Amazon	Black PLA Filament	2	$22.99
HomeDepot	Zinc Plated Machine Screw	2	$1.24
HomeDepot	Flexible Pipe Cap with Clamps	1	$4.98
HomeDepot	Stainless Steel Hex Nuts	1	$1.38
GetFPV	T-Motor F90 2806.5 Motor - 1500KV	6	$29.99
Amazon	8040 Glass Fiber Nylon Propellers 8 Inch	2	$19.99
Amazon	Swan Mineral Oil 16 oz	1	$8.69
Amazon	Anti Vibration Pads	1	$13.80
Amazon	Amazon Basics Electrical	1	$11.18
Hometown	FAA Regulation Lights	5	$3.99
Amazon	Bluetooth Hygrometer Thermometer	1	$14.98
Total Cost Breakdown			
Total Cost			$1120
Remaining Budget			$380

Table 1: Budget Breakdown.

1.6 Societal Impacts

The implications of an AUV are far reaching and could affect many different industries. Currently there is a stringent separation between underwater vehicles and aerial vehicles, both being designed in a completely different way. Both UAVs and UUVs share a similar function, an autonomous vehicle traveling through a fluid. By designing an AUV with this principle in mind we are meshing the world of aerial vehicles and underwater vehicles to create something that has high versatility and adaptability. An unmanned vehicle that can travel through air and water opens many possibilities for industry and national security.

An example of AUVs effecting industry could be the use of AUV for the inspections of offshore oil rigs. Active and retired oil rigs both require inspections to check structural stability and the condition of the oil well itself underwater. Inspecting supports, beams and the underside of an oil rig can easily be done using a quadrotor with a camera, allowing for detailed inspections of hard-to-reach areas. Underwater oil wells and subsea pipelines often require inspections as well, often completed with either UUVs or divers. Utilizing an AUV the complete inspection of an oil rig can be completed at once with a single autonomous vehicle. In addition to that an autonomous vehicle like this could be stationed on a retired oil rig and could routinely run inspections of the rig and recharge all with no human interaction.

AUVs could have a wide impact on nation security as quadrotors are already such a critical part of the armed forces. Small AUVs like the one this MQP team is developing could be essential technology for reconnaissance and security. Being amphibious allows this quadrotor to surveil both above and below the waterline, making it ideal for locating vehicles or obstacles. The quadrotor could also complete a full inspection of a boat's hull above and under the waterline, eliminating the need for dry-docking.

2 Background

2.1 Brief History

Unmanned aerial vehicles (UAVs) are unpiloted aircraft controlled autonomously, remotely, or a combination of both. They operate using a combination of sensors, receivers, and transmitters to monitor their flight and receive and send various signals. The earliest UAVs were known as remotely piloted vehicles (RPVs), and they were first used during World War II. These UAVs (or RPVs) were large and mainly used for military applications such as surveillance, communication, or delivering offensive ordnance. After the 1980s and the introduction of the Global Positioning System (GPS) in 1973, UAVs began to use sensors that could monitor their live position and guide their flight [1].

UAVs can be classified under fixed wing, rotary wing, or flapping wing. A quadrotor is an example of a rotary wing UAV, see Figure 2.

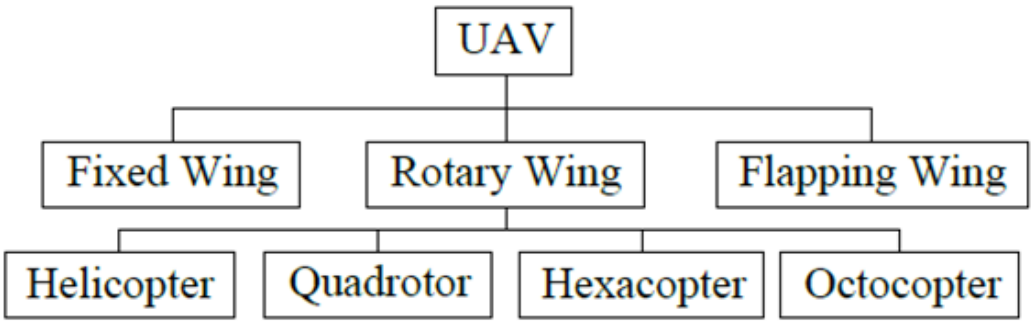

Figure 2: UAV Classification Chart [2].

In addition to UAVs, AUVs have been under active development since the early 2000s and can operate either fully or partially autonomously while remaining unmanned. AUVs have begun to show promising applications in urban surveillance, agriculture, media coverage, logistics, deliveries, and flying taxis or ambulances [3].

For this project, a GPS-denied AUV was developed using a quadrotor design. Quadrotors are less susceptible to air turbulence than fixed wing aircraft and have high maneuverability and small size, making them easier to control than other types of rotary wing vehicles. They are widely used in both civilian and military applications and are controlled by adjusting the rotational speed of its four rotors [2].

2.2 Literature Review

The first built hybrid air to water vehicle was created by Bruce Reid in the 1960s. It was a single-seat submarine called the Reid Flying Submarine (RFS-1). The submarine started in the air at an altitude of 10 meters and then could submerge underwater for 2 meters. More recently DARPA funded a Lockheed Martin project in 2006 to build the Cormorant, a multi-purpose aerial vehicle, MPUAV. The objective was to launch the vehicle from a submarine and carry a 450 kg payload out of the water, and then use jet propulsion to fly. The project was cancelled in 2008, before the vehicle was ever manufactured [4].

Closer to the scope of our project, Professor Francisco Javier Diez at Rutgers University developed a submersible quadrotor named the *Naviator*. The project began in 2012 and launched in 2017 [5]. This quadrotor is a coaxial quadrotor that lands in the water and uses its back propellers to tilt forwards for underwater movement. In 2023, another team of WPI students designed an AUV for this project, the first iteration, dubbed the *Poseidron*. This AUV used a ballast system to pitch underwater instead of propellers, but otherwise followed a similar model to the Naviator. This project was completed with the recommendations from the Poseidron project, and these recommendations are mentioned throughout the document.

2.3 Flight Dynamics Background

2.3.1 Coordinate Systems

The motion of the AUV is described using two distinct coordinate systems. One is the Navigation Frame, which serves as an inertial frame fixed in space at the poolside level. We can define this reference frame as inertial since the accelerations due to the rotation and translation of the earth are negligible compared to the accelerations of the AUV. To simplify matters, we define the X and Y axes to align with the longitudinal and lateral directions in relation to the swimming pool, while the H axis points upwards, representing the height above the poolside surface. The second coordinate system is the Body Frame, which remains attached to the AUV's center of mass, moving, and rotating along with the vehicle. A body-fixed reference frame is necessary as the aerodynamic forces act on the AUV and IMU sensors (gyroscopes and accelerometers) measure quantities relative to the body-fixed reference frame. These coordinate frames are visually illustrated in Figure 3 for reference.

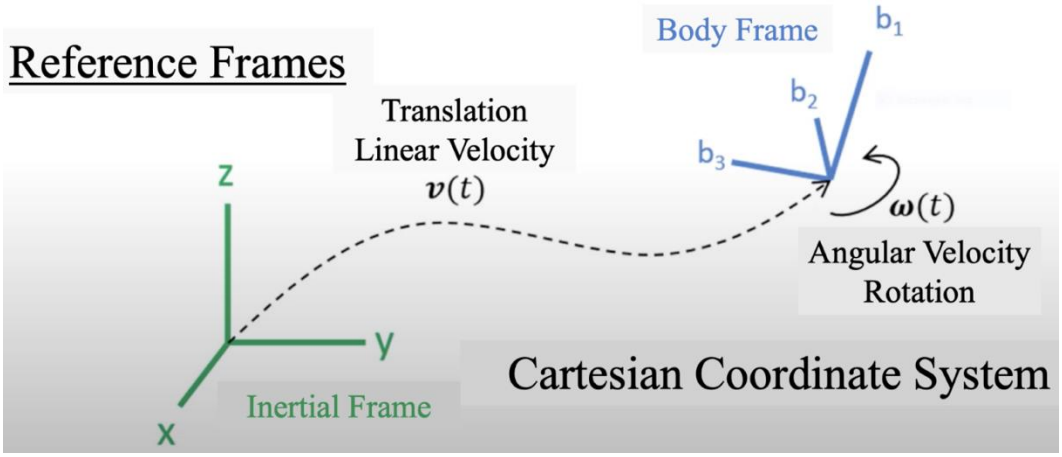

Figure 3: Coordinate Systems for AUV Motion: Navigation Frame and Body Frame [6].

2.3.2 Quadcopter Flight Mechanics

Control over the AUV's orientation, which includes roll (ϕ), pitch (θ), and yaw (ψ), as well as its position in terms of up-down (b_3), left-right (b_2), and forward-backward (b_1), can be

achieved by adjusting the speeds of its four motors. The forces acting on the AUV primarily consist of thrust, drag, and gravitational forces, while the moments are associated with pitching, rolling, and yawing. The AUV's propellers are defined by top-right (1), bottom-left (2), top-left (3), and bottom-right (4). Propellers 1 and 2 will spin in the same direction, clockwise, and propellers 3 and 4 will spin opposite of 1 and 2, counterclockwise. This configuration ensures the two moments generated by motors 1 and 2 (acting in the counterclockwise direction) will cancel out the two moments generated by motors 3 and 4 (acting in the clockwise direction).

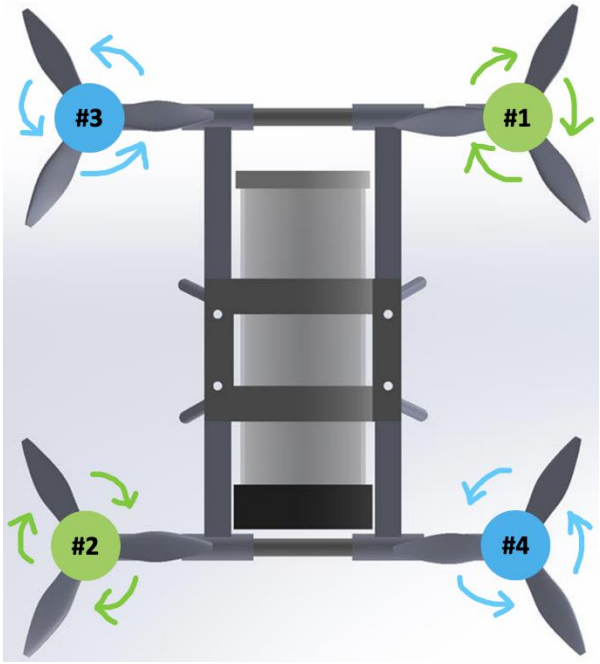

Figure 4: Direction of AUV's Motor Spin during Aerial Flight.

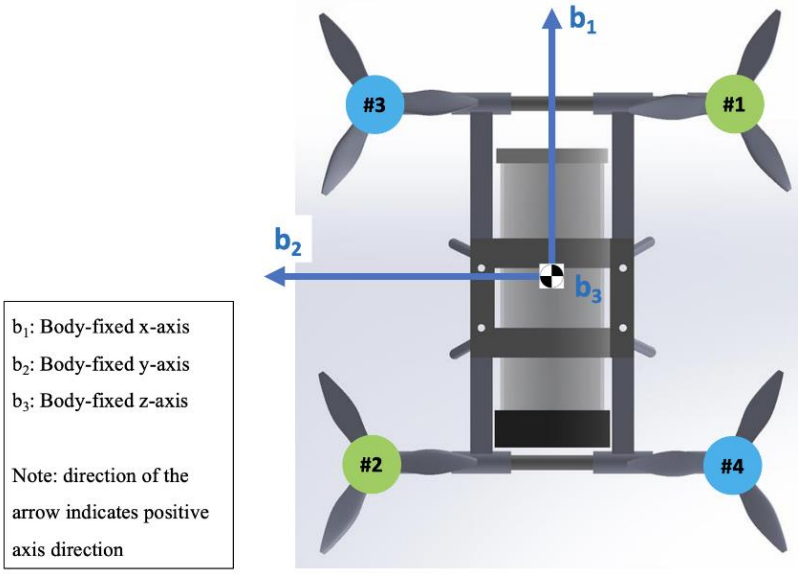

Figure 5: Body-fixed Reference Frame.

To control vertical movement, the AUV relies on all four motors working in unison. When the AUV needs to ascend, it accomplishes this by increasing the revolutions per minute (RPMs) of all four motors simultaneously. Conversely, when the objective is to descend, the AUV reduces the RPMs of all four motors in a coordinated manner. This synchronized adjustment of motor RPMs senses that the AUV moves smoothly and predictably in the desired vertical direction, allowing for precise control of its altitude.

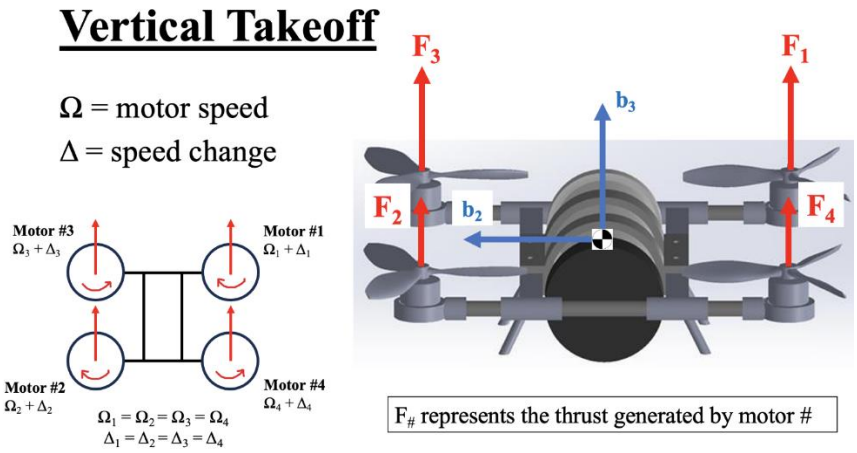

Figure 6: Motors' angular velocity rates and thrust magnitudes for vertical takeoff.

Changing the pitch angle of the AUV involves a coordinated adjustment of the propellers' RPMs. Specifically, to alter the pitch angle, one set of propellers, either 1 and 3 or 2 and 4, must increase their RPMs while the other two remain unchanged. When propellers 2 and 4 have increased their RPMs while propellers 1 and 3 remain constant, it leads to a positive pitch. Conversely, if the RPMs of propellers 2 and 4 remain constant while those of propellers 1 and 3 increase, it results in a negative pitch. This precise manipulation of propeller speeds allows for controlled changes in the AUV's pitch orientation, contributing to its maneuverability in flight.

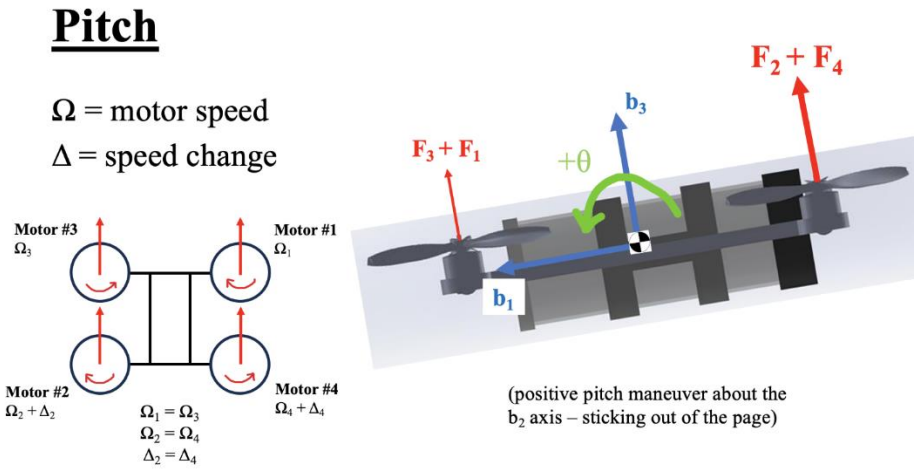

Figure 7: Motors' angular velocity rates and thrust magnitudes for pitch maneuver.

To alter the roll angle, or bank angle, of the AUV, a coordinated adjustment of the propellers is necessary. Specifically, changing the roll angle involves increasing the RPMs of the left propellers (2 and 4) or the right propellers (1 and 3) while decreasing the other sets RPMs. When propellers 2 and 4 on the left side increase their RPMs while propellers 1 and 3 on the right-side decrease, this induces a positive roll. Conversely, if the RPMs of propellers 2 and 4 decrease while those of propellers 1 and 3 increase, it leads to a negative roll. This precise control over propeller speeds enables the AUV to execute controlled roll maneuvers, enhancing its maneuverability and versatility in flight.

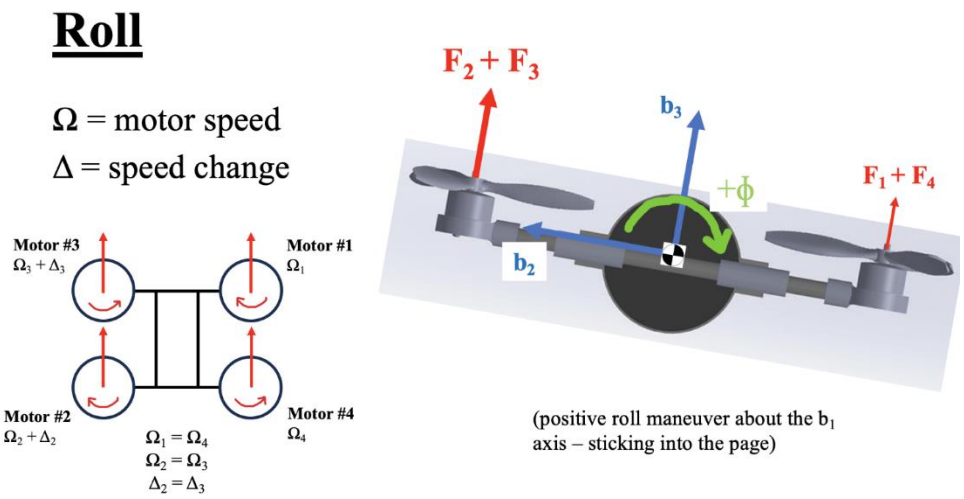

Figure 8: Motors' angular velocity rates and thrust magnitudes for roll maneuver.

Modifying the yaw angle, which affects the heading angle of the AUV, necessitates a specific adjustment of the propellers. To change the yaw angle, the RPMs of the diagonally opposite propellers, either 1 and 4 or 2 and 3, must increase while the RPMs of the remaining two propellers decrease. When propellers 1 and 2 experience an increase in RPM while propellers 3 and 4 simultaneously decrease or remain constant, it induces a positive yaw. Conversely, if the RPMs of propellers 1 and 2 decrease or remain constant while those of propellers 3 and 4 increase, it leads to a negative yaw. This precise control over propeller speeds facilitates controlled changes in the AUV's yaw orientation, contributing to its agility and navigational capabilities in underwater environments.

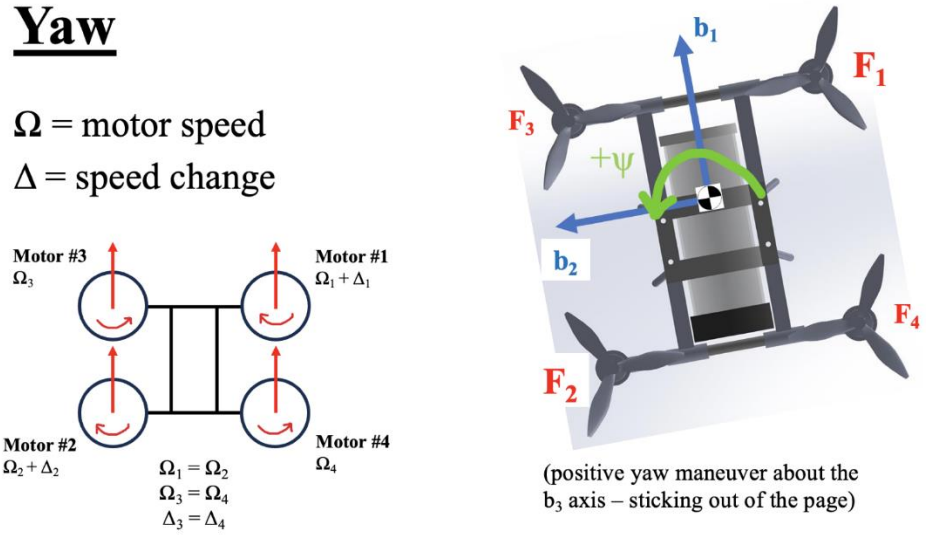

Figure 9: Motors' angular velocity rates and thrust magnitudes for yaw maneuver.

2.3.3 Equations of Motion

Understanding the maneuverability of an AUV requires the comprehension of two distinct principles: aerial and underwater dynamics. The aerial equations of the motion for a quadrotor have undergone extensive research, resulting in well-established and well-documented models. Similarly, traditional underwater autonomous vehicle motion equations have been studied and cataloged. However, our AUV's unique design posed a challenge for deriving the underwater dynamics, as our team found no existing documentation of similar vehicle architecture. Our team derived the equations of motion tailored to this type of vehicle operating underwater. This derivation process closely mirrors the one employed for aerial dynamics but entails the introduction of several critical assumptions.

2.4 Aerial Dynamics

To derive the aerial equations of motion for the AUV, the Newton-Euler method was used. This approach provided a robust framework for understanding and modeling the vehicle's dynamics in the aerial environment. By applying the principles of Newton's laws and Euler's equations, we systematically analyzed and described how the AUV moves and responds to various forces and moments when navigating through the air. This mathematical foundation enabled us to predict and control the AUV's behavior with precision, essential for ensuring stable and accurate performance in aerial operations. The derivation of these dynamics are shown in Appendix A – Aerial Dynamics Derivation.

2.4.1 Aerial Dynamics – Validation

To validate the previously derived aerial dynamics and obtain an approximate RPM rating for each of the motors to perform various maneuvers, the team developed a MATLAB script to simulate the AUV's 12 states during four different maneuvers over a period of five seconds. The script simulates the aerial dynamics of our AUV through a system of ordinary differential equations (ODEs). It begins by defining the time span for the simulation and specifying initial conditions for the AUV's linear and angular velocities, position, and Euler angles. The heart of the simulation lies in the 'system_dynamics' function, which calculates the derivatives of the state variables with respect to time. This function incorporates parameters such as gravity acceleration, AUV mass, and predefined maneuver commands. Based on the chosen maneuver, the script computes RPM values for four motors, subsequently determining motor forces, torques, and distances. The ODEs are solved using the 'ode45' solver, employing a variable-step Runge-Kutta method. The script then generates four figures, each containing three subplots, to visually represent different aspects of the AUV's motion: linear velocity, angular velocity, inertial position, and Euler angles. The results of this script can be seen in Appendix B – Aerial Dynamics Validation Results.

2.4.2 Aerial Dynamics – Analysis

In our aerial dynamics analysis, we delved into the RPM ratings necessary for hovering at different AUV masses; the correlation between additional payload mass and the required RPM rating for each of the four motors; the gradual discharge of battery voltage during hovering; an estimate for the total flight time with varying AUV masses; and an estimate for the total flight time with varying payload masses.

It is crucial to examine the RPM ratings required for hovering at various AUV masses because these ratings directly impact the quadrotor's ability to maintain stable flight. Understanding this relationship allows for precise motor selection and optimal performance.

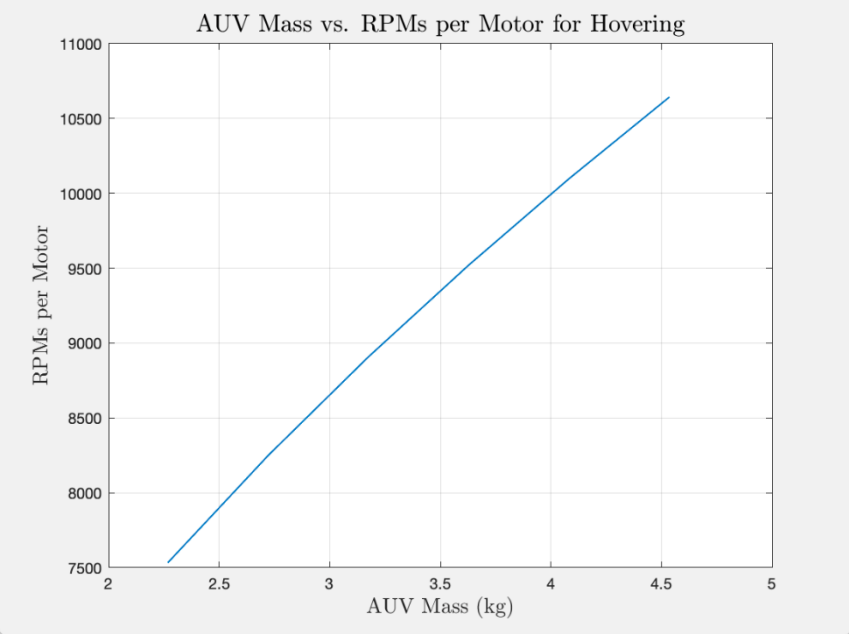

Figure 10: AUV Mass vs RPMs for Hovering.

Exploring how additional payload mass affects the RPM rating for each of the four motors is essential for determining the AUV's load-carrying capacity. This insight guides the design process and ensures that the AUV can effectively handle varying payload weights.

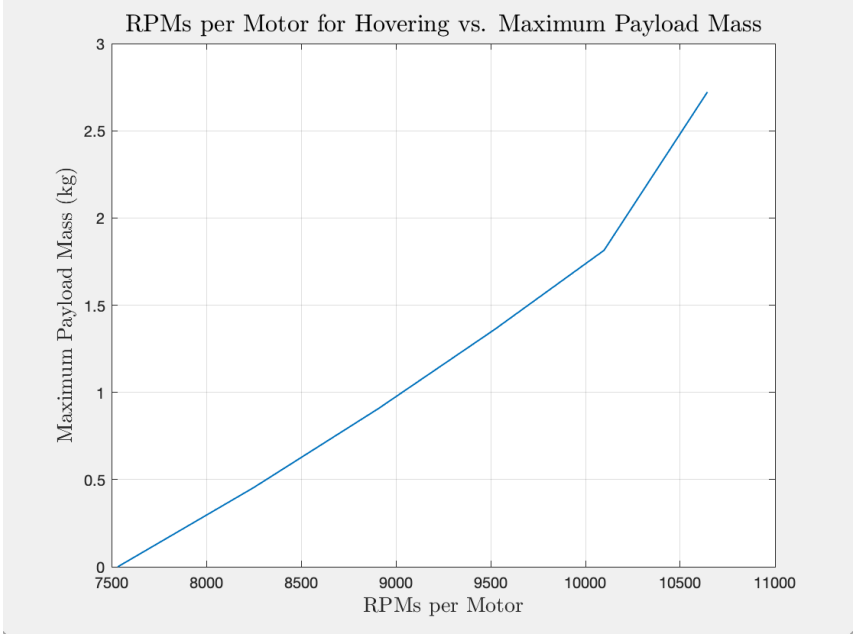

Figure 11:Payload capability as a function of hovering RPM.

Monitoring battery voltage discharge over time during hovering is crucial for assessing the AUV's power consumption and overall energy efficiency. This information aids in designing an efficient power system and estimating the AUV's operational duration.

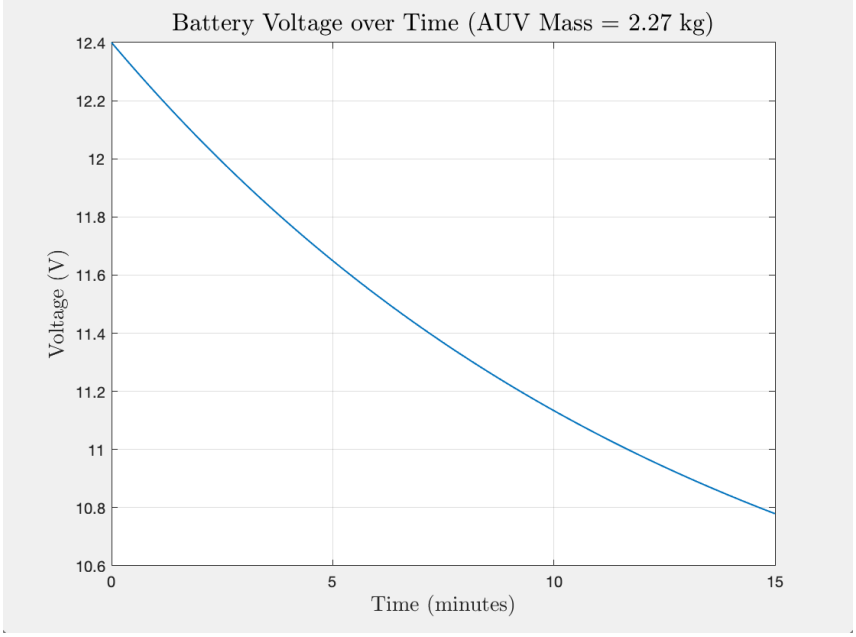

Figure 12: Battery Voltage vs Time.

Considering an approximation for total flight time at various AUV masses is important to anticipate the quadrotor's endurance capabilities under different load conditions. This knowledge is vital for mission planning and optimizing the AUV's performance in real-world scenarios.

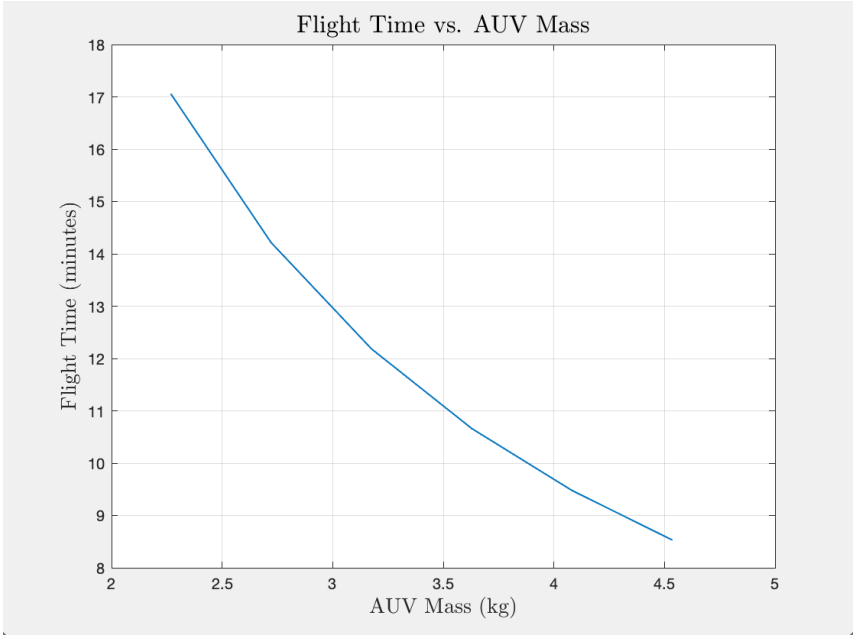

Figure 13: Flight Time vs AUV Mass.

Similarly, contemplating an approximation for total flight time at various payload masses is essential for understanding how different payloads impact the AUV's overall flight duration. This information assists in making informed decisions regarding payload selection and mission execution.

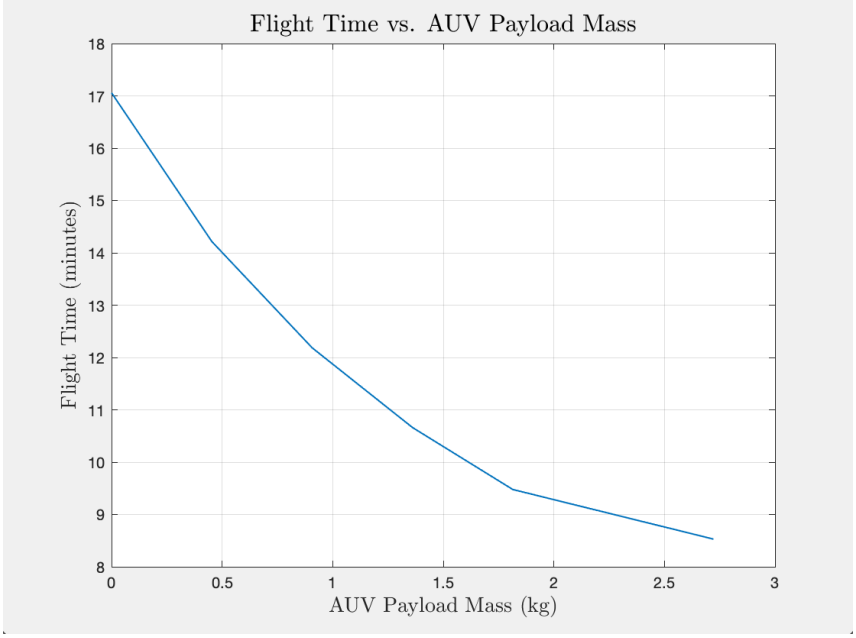

Figure 14: Flight Time vs AUV Payload Mass.

2.4.3 Quadplane Flight Mechanics

Compared to the quadcopter flight mechanics used for aerial flight of our AUV, the quadplane mechanics for underwater locomotion differ. Quadcopter flight mechanics involve the independent control of four rotors to generate lift where quadplane mechanics incorporate a hybrid design of rotors and fixed wings. Quadplanes employ a tilting mechanism for the transition between the two modes, featuring vertical rotors or wings during takeoff and landing and tilting to a horizontal position for forward flight. The versatility of quadplanes arises from their ability to combine the strengths of both rotorcraft and fixed-wing aircraft, offering a broad range of applications that require both vertical and horizontal flight capabilities.

Opting for quadplane dynamics while the AUV is underwater was a strategic decision driven by the striking similarities between our AUV design and the requirements for underwater

locomotion. With integrating quadplane capabilities this allowed the AUV to maneuver underwater.

Figure 15: Direction of AUV's motor spin during underwater flight.

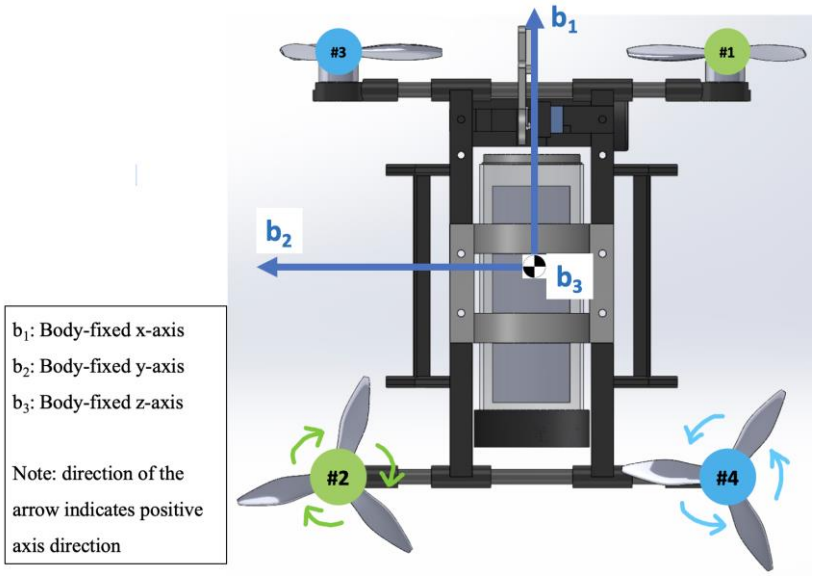

Figure 16: Body-fixed Reference Frame.

The two maneuvers we were hoping to have our AUV perform underwater were propelling forward and pitching. Based on our objective there was no need to perform roll or yaw maneuvers while underwater.

To control forward movement in the positive x-direction of the body-fixed frame, the AUV relies on its two front motors working in unison and its back two motors to control the pitch. When the AUV needs to propel forward, it accomplishes this by increasing the RPMs of the front two motors (#1 and #3) while not powering the back two motors. This synchronized adjustment of motor RPMs ensures that the AUV moves smoothly and predictably in the desired forward direction, allowing for precise control of its position.

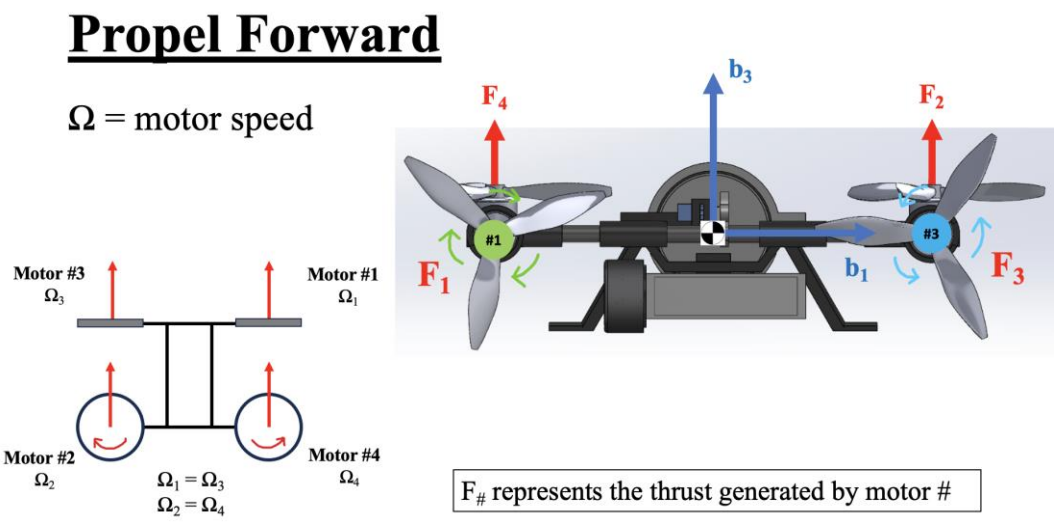

Figure 17: Motors' angular velocity rates and thrust magnitude to propel forward.

Changing the pitch angle of the AUV involves a coordinated adjustment of the propellers' RPMs. To positively increase the pitch angle, the set of propellers, 2 and 4, must increase their RPMs while 1 and 3 remain unchanged. This precise manipulation of propeller speeds allows for controlled changes in the AUV's pitch orientation, contributing to its maneuverability underwater and depth management.

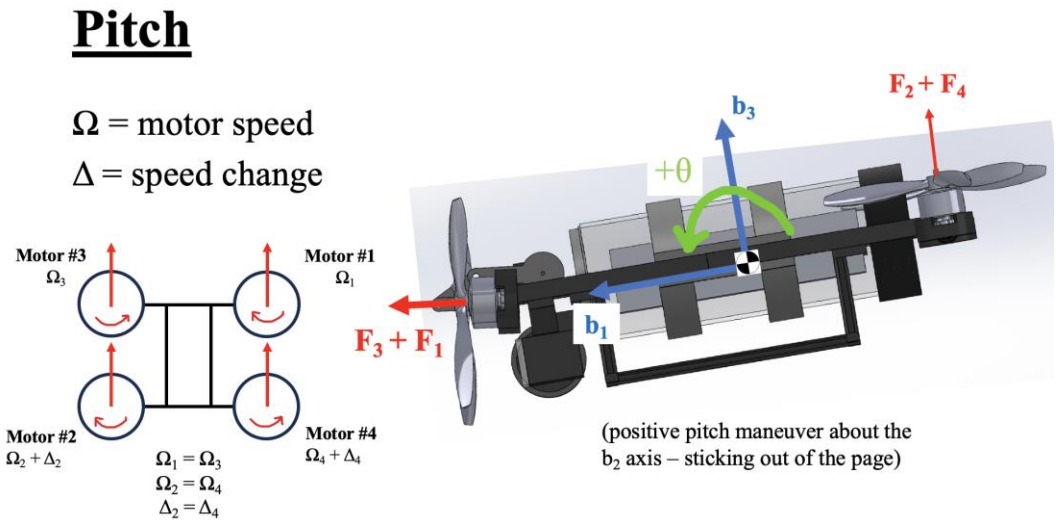

Figure 18: Motors' angular velocity rates and thrust magnitudes for pitch maneuver.

2.5 Underwater Dynamics

To derive the underwater equations of motion for the AUV, the same approach as the aerial dynamics is used, the Newton-Euler method. This method establishes the framework to

comprehend and simulate the vehicle's dynamics in the underwater environment. Utilizing the principles of Newton's laws and Euler's equations, we can methodically examine and articulate the movement and reactions of the AUV in response to forces and moments when navigating through the water. This approach allows us to anticipate and manage the AUV’s actions with precision, a crucial factor for guaranteeing stability and accurate underwater locomotion. The derivation of these dynamics are shown in Appendix C - Underwater Dynamics Derivation.

3 Technical Specifications

3.1 Flight Hardware

3.1.1 Flight Controller

The flight controller is the main computing unit on an AUV, it takes sensor data as input and then uses a control software to send signals to the motors to control the craft. Flight controllers often come with a suite of built-in sensors that allow for the controller to automatically estimate the state of the aircraft without any additional electronics.

When choosing a flight controller for the AUV the team considered:

1. Processing Power
2. Sensor Package
3. Layout

It was important that we chose a flight controller with adequate processing power since we will be heavily relying on it for autonomous flight. In addition to that, the localization system that we are using will be an additional computing burden.

The sensor package on the flight controller was one of the most important considerations that we had. Since the quadrotor will be flying GPS-denied, it is crucial that we have a robust high-quality sensor package. We were looking for high quality IMUs with redundancy, quality magnetometer and barometer. Most important are the IMUs, flying GPS-denied means that IMUs are heavily relied on and with no other localization system, the sensor error will accumulate, and measurements will drift significantly. Ideally, we would like multiple sets of IMUs for redundancy but with a host of other sensors we could make do with just one high quality set.

The layout of the flight controller describes the size, port selection, and compatibility. Ideally, we would like a lightweight flight controller with no exposed circuits to minimize the chance of shorting a circuit with water or static. Next the port selection is important because it determines how many other sensors and systems we can link to the controller. We wanted a controller with lots of varying ports so that we could add sensors or other electronics to the system if needed. Compatibility relates to what software the controller can run and what sensors it is compatible with. In the end we decided to go with the Pixhawk flight controller, this was mainly due to its versatility and availability. The Pixhawk automatically supports GPS-denied localization and our software of choice. In addition to that, the Pixhawk has a robust computing core with up to 4 serial connections.

Figure 19: Pixhawk Flight Controller [7].

3.1.2 Companion Computer

The companion computer is an essential part of an autonomous vehicle, it functions as the highest level of command, essentially the 'brain' of the quadrotor. For the AUV we needed a companion computer that had a USB port, small form factor, and serial connection compatibility. On the AUV the companion computer needed to calculate position data from the camera images, maintain autonomy failsafe procedures, run autonomy scripts, and maintain constant MAVLINK communication with the flight controller. The most common companion computer used in AUVs is the Raspberry Pi which is what this project opted to use. Specifically, the Raspberry Pi 3, which has a very small form factor and all the required ports for the AUV. The Raspberry Pi was flashed with the Raspbian operating system, a light version of Linux.

Figure 20: Raspberry Pi 3 [8].

3.1.3 Power Subsystem

The power subsystem on the AUV encompasses the battery, and power step-downs. When choosing the battery of the quadrotor the three deciding factors are battery type, cell number and capacity. The battery type is the chemical composition of the battery, the most common types being LiPo, LiIo, LiFe, NiMH, NiCd. Cell number refers to the number of cells in the battery which corresponds to the voltage. Capacity is the electrical storage of the battery and determines the battery life of the quadrotor, this is measured in mAH (Mili-Amp Hours). For the AUV we opted to use a LiPo, 3 cell 11.1V, 5200mAH battery as it was already available from the previous MQP and fitted our needs perfectly.

Figure 21: LiPo Battery.

Choosing the power step-down units depended directly on the electronics that needed to be powered on the AUV. The only electronics that required a smaller controlled voltage were the Pixhawk flight controller, Raspberry Pi, and the tilt servo. For the Pixhawk we opted to get the manufacturer-recommended power unit (5V 2.3A) because it had the correct plug and surge protection. For the Raspberry Pi and tilt servo we used two generic 5V 2.3A UBECs to step the voltage down. The power system is structured as one high-voltage line (11.1V) with the 3 step-downs spliced within, leading to the ESC which distributes the high-voltage to the motors.

Figure 22: UBEC Power Step-Down.

3.1.4 Propulsion Subsystem

The propulsion subsystem includes the motors and ESC (Electronic Speed Controller). Choosing the components for the propulsion subsystem requires an initial guess of weight so that the correct motors can be chosen. Once we decided on an initial weight guess motors could be chosen.

The deciding factors when choosing motors are stator size and kV. Stator size is the width of the coils within the motor, which determines the overall power that the motor can produce. kV is a measurement of the torque of the motor which also corresponds to the maximum RPM that the motor can produce. During the build phase of the project two different motors were tested with varying success. The first motor we tested had a stator size of 28mm (about 1.1 in) and a kV of 920, we chose this because we believed it would be best to choose a high-torque motor for underwater motion. When testing this motor, we found that it did not produce sufficient RPMs for proper aerial flight and decided to move away from high torque. The next motor we tried was also 28mm stator size but 1500 kV, this motor provided more than enough power for aerial flight so we decided to use it, knowing we would just have to decrease speed when underwater.

Figure 23: 12mm Stator Motor.

Choosing an electronic speed controller depends on the needed amperage of the motors and the function of electronic speed controller. Once the motors were chosen, the ESC amperage could be sized, for both iterations of motors the max draw was around 45 A. The speed controller's function dictates whether it can control multiple motors or only one. Specifically, for the AUV a 4in1 ESC was desirable because of its small form factor and compactness. The only issue with using a 4in1 ESC is that it is not innately compatible with the Pixhawk flight controller, meaning a custom wiring design needed to be created. The ESC chosen was the Velox 45A 4in1 ESC. This provides enough power for all motors and fits well in the small electronics enclosure.

Figure 24: Velox 4in1 ESC.

3.1.5 Sensing and Localization Subsystem

The sensing and localization subsystem includes all sensors the AUV uses to estimate its state. On most quadrotors, these are the internal sensors of the flight controller and an external GPS. On the AUV GPS half of the sensors in the flight controller are not viable for estimating the state. The Pixhawk flight controller includes IMUs (Inertial Measurement Units), a magnetometer, and a barometer, while underwater or indoors the barometer and magnetometer are unusable, leaving only the IMUs. To add more accuracy to the sensor, package a localization system needed to be added. Potential options for localization are motion sensors, radio frequency positioning, and tracking cameras. Motion tracking could not be used because it would lose track of the quadrotor once underwater, and the radio frequency positioning would be hard to implement in a quadrotor, especially for both aerial and underwater. Tracking camera technology was chosen because a tracking camera was bought by the previous MQP and was somewhat compatible with the chosen flight software.

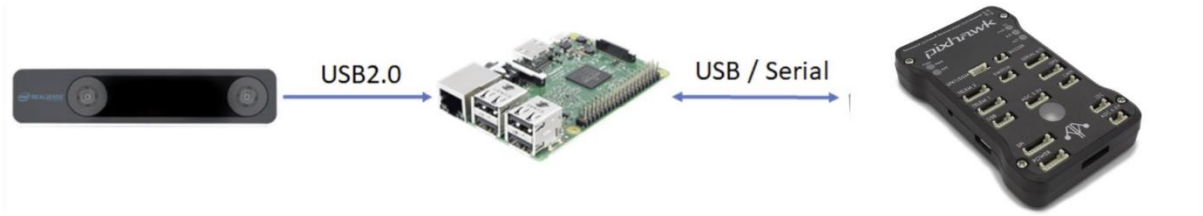

Figure 25 Intel T65 Tracking Camera to Pixhawk [9].

We ended up using the Intel T-265 tracking camera which uses a dual fisheye camera to estimate the six following data points in a local northeast down coordinate system: Velocity in X, Y and Z, and position in X, Y and Z. This data is calculated onboard the camera with the internal processing unit, it is then sent to the Raspberry Pi via USB 2.0. On the Raspberry Pi, the data is transformed with the correct camera orientation and offsets, the data is then sent to the flight controller via a serial connection using MAVlink (Micro Air Vehicle Messaging Protocol). Since the flight controller can only use the IMUs of the board sensor suite, the parameters in the autopilot software have been changed to use the camera heading as default. The autopilot also uses concepts of multisensory fusion to combine both the IMU estimates with tracking camera data to create a more accurate state estimate.

3.2 Software

3.2.1 Ardupilot & Frame Type

ArduPilot is a free open-source software design for operating rovers, copters, planes, and submarines. This software is widely used in both academic/research and commercial settings. Its versatility in supporting different platforms and robust controls architecture makes it one of the most popular autopilot software's available. For this project we used two different versions of ArduPilot, ArduCopter and ArduPlane.

ArduCopter is a version of ArduPilot that is meant to control any type of copter, single helicopters to octocopters. We initially used ArduCopter to test the AUV in aerial settings so we could validate that the frame and motors worked. The AUV was running in this software for the first 14 weeks of the project, until work on autonomous submerged flight began.

When working to make the AUV work submerged, we uploaded the ArduPlane software, which is meant for aerial flight of planes. We chose to use this software for the final version of our project because there is a very specific frame type on ArduPlane that this project could take full advantage of Quad-Plane mode. This is a frame type with a prebuilt controls architecture that allows for a vehicle to transition between a VTOL frame into a plane with forward facing propeller by utilizing a servo to tilt the front motor axis. Although this software was meant for VTOL planes, we were able to adjust settings and parameters within the autopilot to throttle

while in plane mode to account for a denser liquid, i.e. water. By adjusting these settings, we were able to use aerial plane dynamics for submerged flight, since both domains are liquids, one is just significantly denser.

3.2.2 MAVLink

MAVLink stands for Micro Air Vehicle Communication Protocol, it is a standard for small unmanned aerial systems, it is used for most small AUV variations of it even being used for larger commercial and government platforms.

It is a basic protocol that relies on sending a message and receiving a confirmation from the platform. Specifically in this project MAVLink was used for communications via 955 MHz telemetry radios between the AUV and a ground control station running the Mission Planner ground control software. MAVLink was also utilized for serial connection communication between the Raspberry PI and the Pixhawk flight controller. MAVLink is crucial for the control of the Vehicle because it allows for the wireless monitoring of the AUV's telemetry data, and also for the communication of movement commands to allow for customized autonomous flight.

To read and write MAVLink messages this project utilized the python packages Pymavlink and DronekitAPI. Pymavlink is a low-level python wrapper that allows for the writing, encoding, transmitting, receiving, and decoding of MAVLink messages. DronekitAPI is a high-level package that utilizes Pymavlink to send general commands to the AUV using simple functions, it also allows for easier use of local coordinates and reactive autonomous flight.

3.2.3 Autonomy Scripts

In order for a multi-domain autonomous mission using ArduPlane, it was critical to write custom autonomy scripts to cater to the very specific scenario the AUV would be in. ArduPlane and the Mission Planner ground control software have prebuilt autonomous mission frameworks, but they rely on waypoint systems that must be uploaded prior to a mission and cannot be dynamically changed during the mission due to unforeseen variables.

For this project the companion computer was used to house a set of scripts that dictate autonomous flight. To write these scripts python and the aforementioned python packages were used. The general layout of the scripts are as follows, a low-level data manager script, a mid-level function housing script, and a high-level autonomous mission script that details the specific mission required of the AUV.

The low-level data manager script focuses on establishing a serial connection between the flight controller and the Raspberry PI, carrying out basic transmission and reception tasks, and populating a local database with flight telemetry. The script uses another package called Redis, which is a database package. This script is continually requesting telemetry data via MAVLink from the flight controller, once receives it updates the local Redis database with live flight data.

The mid-level function script acts as a repository of functions and actions that AUVs can take. The point of this script was to decrease the volume of code used in the final autonomy script and make writing/altering autonomous mission easier for the final user.

The high-level autonomy script as a final mission framework, building off of the functions from the other two scripts it is relatively easy to compile an autonomous mission. Using the live-flight data from the Redis database, decisions can be made during the mission to alter the flight path.

In addition to the main autonomy scripts there is another script used as a failsafe to ensure that the AUV will not lose control. This script is mainly meant for submerged flight as radio transmission below the water is difficult past 1ft of dept. The autopilot software will automatically revert to default failsafe procedures should RC transmitter signals are lost, meaning it will try to hold a steady position as if it were in the air. This is a high problem because the propeller will spin at nearly full speed, propelling the AUV in an uncontrolled motion underwater. This script uses the local Redis database on the Raspberry PI to monitor the RC channels being received and once they are nonexistent, the script will repeatedly send disarm commands to the flight controller.

3.3 Control System Architecture

To ensure GPS-denied flight, care had to be taken to ensure the control system was accurate enough to complete the mission parameters. The system can be described in twelve states: linear position and velocity in three dimensions, and angular position and velocity in three dimensions. The Intel T265 tracking camera was integrated into the system to increase accuracy in measured states to ensure the AUV followed the predetermined path. The final system consisted of an IMU and MPU in the Pixhawk flight controller, and an IMU and VPU in the tracking camera. The IMUs (intertial measuring units) consisted of accelerometers and gyroscopes. These sensors measure the linear acceleration and angular velocity, respectively. Note that to measure linear velocity, the linear acceleration terms needed to be integrated, which over time adds uncertainty to the system. The VPU (visual processing unit) on the tracking camera takes linear and angular position data. With this array of sensors, the control system measures all twelve states of the system.

ArduPilot’s software uses a PID (Proportional-Integral-Derivative) feedback controller. This controller allows for a feedback-based closed-loop system to ensure the most stability in control of the AUV, especially important in this case as the system operates autonomously. A simplified diagram of the controller can be seen in Figure 26. This controller takes target angles from the autopilot and measured angles from the sensors and determines an error between the two. This error passes through a square-root controller which determines the rate necessary to minimize the error. This data is then sent to a lowpass filter which removes the high frequency values of the error, further increasing the clarity in the data. Next, the error between the new desired rate and the measured rate is determined, and again sent through a lowpass filter. Then the PID controller which determines the control signals to pass to the motors to reduce the error in the rate. Then the measured data is sent back to the beginning, completing the loop. Note the

"IMAX" term on the integral term of the PID. This is an effort to reduce what's referred to as integral "wind-up". This is when the integral term grows unachievably large as error is sustained over long periods of time. This often leads to overshooting in the system. The "IMAX" block ensures that the integral term remains under a certain value to not allow this "wind-up".

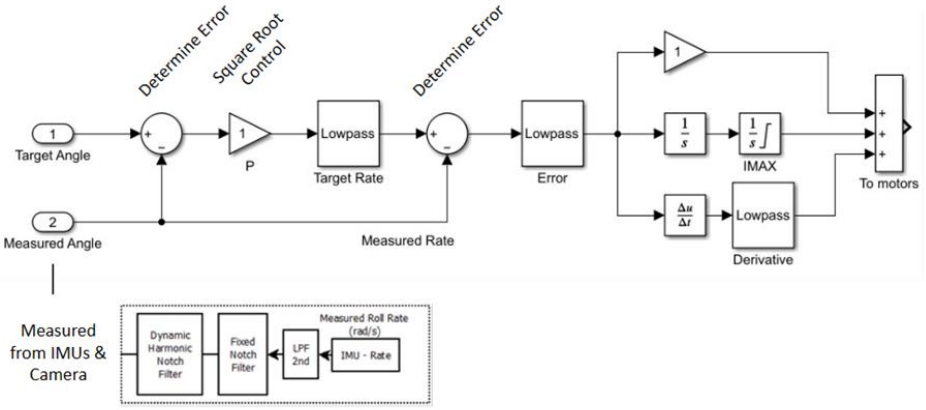

Figure 26: ArduPilot Control System Breakdown.

The sensor data that comes into the controller is inherently "noisy", meaning the measured signal is not exactly what is being measured. The ArduPilot cuts back on this signal noise using Extended Kalman Filters (EKFs). The software runs several EKFs in parallel and records the uncertainty in each measured signal. Since the system has redundant sensors, the EKF system is programmed to use the measurement from the sensors with the lowest uncertainty. This switches as uncertainty increases or decreases for different sensors, but only uses one of each redundant sensor at once [10].

3.4 Quadrotor Body Design

3.4.1 Quadrotor Frame Design

Initially, a tri-rotor style frame was considered, this was intended to minimize drag underwater given the switch to the tilt-rotor function for underwater propulsion. However, the tri-rotor concept was dropped in favor of using a quadrotor due to concerns about its controllability in an aquatic environment. Specifically, there would be lack of ability to control the roll of the vehicle while underwater due to the tilt-rotor function gimballing the front two motors for use as forward propulsion. In normal flight these two motors would be entirely responsible for controlling the roll angle as the third motor was located along the vehicle's centerline, and thus has no ability to influence the roll behavior. With a quadrotor frame all four motors control the roll behavior, and with the tilt-rotor function there would still be two motors capable of controlling roll in underwater environments. Another major consideration in the decision to switch to a quadrotor design over a tri-rotor was the comparative amount of existing information available on the specifics of the dynamics and controls of such a vehicle. This was largely due to the overwhelming comparative popularity of quadrotors amongst both commercial quadrotors and hobbyist AUVs. This was important as the underwater dynamics of the vehicle would need to be derived due to the novelty of the tilt-rotor approach to underwater propulsion.

For this reason, having an abundance of relevant resources to reference was considered preferable.

Although quadrotor frames of all sizes are commonly available in an X-style frame configuration, it was determined that an H-style configuration would be preferable for this project. This was because it would greatly reduce the required complexity of the mechanism for actuating the tilt rotor function. Instead of each of the two front rotors being tilted independently, the structural member that they were both attached to could be rotated. This would require only a single mechanism and would ensure that both rotors remained aligned with each other at all times, reducing dynamic and controls complexity and minimizing possible failure modes resulting from this aspect of the design. Although H-style frames are less commonplace among commercially available quadrotors, they do not differ in any notable way from X-style frames with respect to their controls and dynamics. This means that there would be no added complexity to the design or controls resulting from this decision.

3.4.2 Enclosure and Flight Hardware Positioning

One of the project's complexities was the need to consider the vehicle's hydrostatic behavior alongside the stability in air. In an aquatic environment the buoyancy of certain components or areas of the quadrotor would be one of the primary factors influencing its stability, while in the air the only concern in this regard would be the center of mass. This was made a complex issue because some of the heaviest components, the waterproof enclosure and flight hardware, were also likely to be the most buoyant components in the vehicle. This imposed some challenges in terms of determining the positioning of this enclosure relative to the rest of the vehicle to optimize the stability of the quadrotor in both principal environments. Traditional quadrotor design suggests that the center of gravity be as low as possible to enhance stability during flight. Meanwhile, the center of buoyancy should be kept as high as possible to enhance stability underwater. As these options are mutually exclusive and choosing one would negatively impact the stability in one of the environments, it was decided that the enclosure should be positioned vertically in-line with the main structural members and the motors, to minimize the impact its positioning would have on the center of mass and buoyancy. This would also enable easier tweaking of stability and buoyancy using the addition of small weights and flotational elements as ballast.

3.4.3 Material Selection

Multiple materials were considered as options for various parts of the vehicle’s structure. These options included carbon-fiber composites, fiberglass, various plastics, and 3D printing material. Carbon-fiber parts were a viable option due to their extremely high strength to weight ratio and stiffness. Another aspect that made carbon fiber attractive was that it was not an uncommon option for the structure of commercially available quadrotors frames. This meant that if the design could be made to fit a preexisting frame, a significant portion of the vehicle’s structure could be made using a relatively high-quality material. Fiberglass was also considered for many of the same reasons as it has relatively high strength and rigidity at a fraction of the weight when compared to other materials. Another advantage of using fiberglass was some

members of the group had prior experience with fabrication, and access to resources to create an enclosure. Lastly, various methods of 3D printing parts were considered, the quality of the parts depend heavily on the type of filament and the printing method used. The group had access to various 3D printing resources outside of the ones offered by the school, which allowed for consistently rapid prototyping of 3D printed components and enabled the creation of relatively strong printed structural parts.

A mix of materials were chosen to create a frame based on the requirements for the structure. Most of the frame was created using 3D printed parts which allowed us to fully customize the frame and accomplish our unique objective. The three types of 3D printing material the team investigated were resin, ABS and PLA filament. One reason the team decided to use PLA filament is because it has a higher tensile strength than ABS and resin. This was important because we needed a strong frame that could carry our electronics that would not break if a malfunction occurred, and it crashed. Another important aspect the team considered was the time it would take to manufacture a part. Our team did not want the project to face delays due to parts not being able to print. Printing parts in resin would take considerably more time and would not have allowed us to iterate our quadrotor frame as quickly. Our design also incorporated carbon fiber rods for the motor arms. These rods provided them with a strong foundation for the motors to be mounted on and allowed us to gimbal the front access.

The team used a combination of commercial nuts and bolts to assemble the AUV frame. Commercial hardware is widely available, cheap, and extremely reliable to hold our parts together. This also allowed us to easily disassemble the frame and get access to the electronics, which was important when we started to test the AUV frequently.

3.4.4 Electronic Enclosure

Through our conversations with the previous year’s MQP team, they advised that we move away from 3D printed enclosures due to their troubles with waterproofing. Instead, they recommended that we investigate commercially produced products or other concepts. Through our research and discussions, our team narrowed the options down to three different enclosures. The main factors that the team considered were waterproofing, accessibility to electronics, and cost. Implementing an enclosure that we can rely on to safely keep our electronics dry was one of the team's highest priorities during our flight underwater.

The first option that the team considered was a watertight enclosure from the company BlueRobotics. This company is known for selling accessible, reliable, watertight enclosures for robotic underwater vehicles. Their products offer a wide variety of enclosure diameters and end caps including a dome and an end cap with cable penetrators. Based on the pricing available on their website, this enclosure would cost around $400 to $500, which is a third of the team's total budget.

Figure 27: BlueRobotics Enclosure Options [11].

The second option that the team considered was creating a fiberglass enclosure. This would involve creating a mold, then laying up the pre-woven sheets and saturating them with resin. This was determined to be a viable option due to the prior experience of some group members with similar processes and the resources and facilities available to said group members. It was determined that the best method of running wiring through this type of enclosure would be to run them through during the layup process. Having the wiring integrated into the laminate construction would likely result in a more robust seal than drilling holes after the fact to run them through. This idea wasn't examined to the point that a complete cost analysis was carried out, as it was determined that other options would likely be more or as effective and cheaper.

The final option the team discussed was an enclosure made from PVC piping, sealed at both ends using commercially available heavy-duty rubber test caps intended for the use with such piping. Wiring would be run through holes drilled in these end caps and made watertight using 5200 Marine Adhesive. The specific adhesive was chosen based on research of methods utilized for similar applications. It was determined that this enclosure would cost around $60 in materials and would likely achieve the same level of watertightness as the other options, with the only question being the robustness of the wiring seals. It also would offer easy removal of the components for maintenance, as the end caps were intended to be relatively easy to take off.

It was ultimately decided that the third option would be ideal. It was by far the cheapest option, which was desirable given the budget limitations of the project. It also offered waterproofing comparable to that of the other more expensive options and left open the option

for replacement of components of the enclosure due to potential damage during testing or changes in plans or requirements later in the design and testing process.

3.4.5 Camera Enclosure

As the Intel T265 camera needed to have a clear, unobstructed view forward of the vehicle, it was determined that the camera would need to be contained in a separate enclosure from the main one which housed the rest of the flight hardware. This enclosure would also need to be completely watertight and would also need to offer a clear view for the camera, free of visual obstructions or distortions to allow the camera to provide accurate tracking data. Lastly, the enclosure had to allow for easy removal of the camera for maintenance purposes.
Due to the unique shape of the Intel T265 camera, our options for watertight enclosures were extremely limited. There were no commercially produced products specifically designed for this model which led to the decision to fabricate something ourselves.

The first option the team considered was creating a second PVC enclosure like the main enclosure holding the rest of our electronics. Since the camera lens could not be distorted, using a circular PVC pipe was not an option. This led the team to consider a less common, square shaped PVC pipe. Due to the limited quantity of options available, the smallest PVC enclosure we could get was 2 x 2 in. This was much larger than our camera, which was not ideal. Having too large of an enclosure on the front of the quadrotor would increase drag and cause the quadrotor to not be neutrally buoyant. With these concerns the team decided to investigate alternative options.

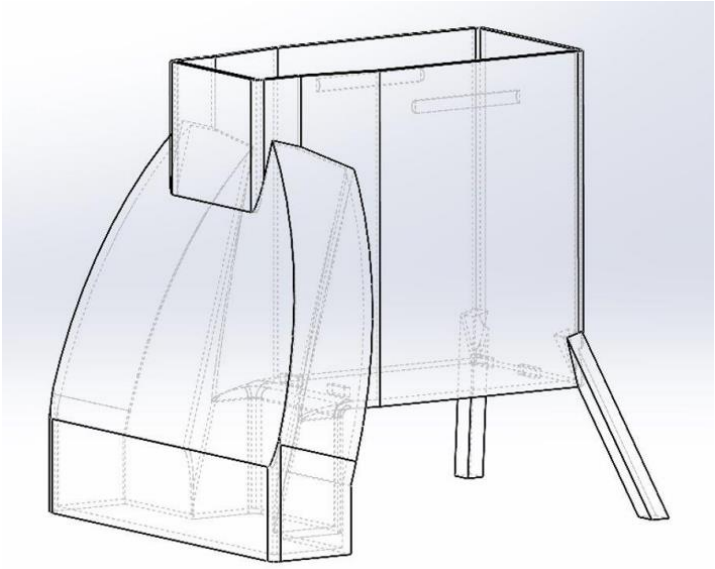

Figure 28: Poseidron Team's Electronic Enclosure V2 [12].

The option we chose was to create a custom 3D printed camera enclosure. This option gave us more flexibility in creating an enclosure specifically for the Intel T265. One obstacle that

the team would have to overcome was in waterproofing. Through some discussions with the previous MQP team, they attempted to create a 3D printed enclosure to store the electronics and camera but ultimately failed due to the concerns with making it watertight. The second version attempted to solve some of their earlier issues by minimizing the needed supports and joints while allowing the enclosure to be simplified into one piece. Since the height was increased to house all the electronics, more layers were used to print the enclosure which caused small holes to form along the walls. To overcome this issue, the team applied a waterproof commercial spray for the testing. For additional protection a rubberized paint sealant was applied over the spray. This approach was successful in patching the holes between each layer of filament. One area they could make watertight was the bolt pattern assembly. Even with multiple iterations they could not fully seal the assembly with the flange and gasket design.

Figure 29: Waterproof Camera Enclosure.

For our design, our goal was to keep the design simple and utilize similar practices that worked with the electronics enclosure. This design incorporated a one-piece 3D printed enclosure, a rubber gasket with a hose clamp, acrylic, flex seal, 5200 marine adhesive, and dampening foam. By making the enclosure one piece, we would avoid the issue the previous MQP team faced with the bolt pattern assembly. Instead, we accessed the camera using a 1-inch rubber gasket with a hose clamp. This rubber gasket has multiple O – rings inside to keep water from getting in and can be tightened with the hose clamp. Our team followed the same process as the previous MQP in using Flex Seal to make the 3D enclosure watertight.

3.4.6 Tilt Rotor Design

During the early stages of our project, our team discussed two different ways the quadrotor could move underwater. The first option was to build off the previous team's design using a ballast system. The ballast system provided advantages in two primary aquatic settings.

When the ballast was empty the quadrotor would float vertically due to the center of mass and center of buoyancy being aligned. The second scenario was when the ballast was 75% full, the quadrotor's center of mass and buoyancy were aligned in the horizontal direction. Even with these advantages, their team recommended removing the ballast system for future projects. Their reasoning was due to the added complexity and weight that it created. The second design we discussed was creating a quad rotor with gimballing front motors. This would allow our quadrotor to fly in air with all motors vertically aligned and when underwater the front two motors would gimbal forward providing horizontal thrust. Our team decided to remove the ballast system from the design based on the recommendation from the previous MQP group.

For our first design iteration the team decided to use two 3D printed gears to rotate the front carbon fiber rod. This design was chosen due to its simplicity and cost effectiveness. By using 3D printed gears, the team could easily iterate the design if there were any concerns that arose. The team implemented multiple different designs using gears. Each time we changed the thickness and the size of the teeth. The problem we faced was the torque produced by the servo was not transferred between the two gears. When we activated the servo, the main gear would rotate, but the secondary gear would not engage. The contact surface of the main gear's teeth was too small to engage the secondary gear causing it to slip.

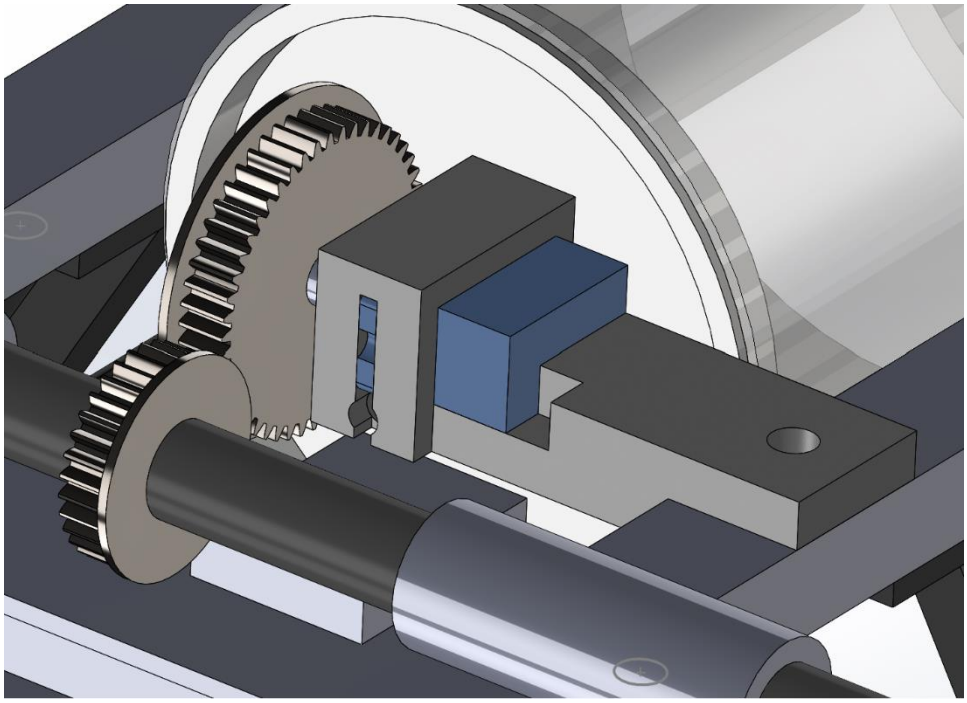

Figure 30: Gear Mechanism Controlling Gimballing Axis.

For the second iteration, our team decided to use a different mechanical mechanism to gimbal the front motors. Our goal was to keep the complexity of the design simple while minimizing the risk of failure in the transition between quadcopter and quad plane mode. Since we had already bought a servo and printed the stabilizing mount our new design would have to incorporate these two components as well.

Our team decided to utilize a three-bar linkage mechanism to gimbal the front motors. In the design we had the base of one bar connected to the servo horn, another bar connected to the gimballing carbon fiber rod, and a third bar joining the bars together. The linkage was secured using a nut and bolt. When underwater the aircraft's maximum gimbal angle was 90 degrees. To accomplish this, we designed the bar connected to the servo and the bar connected to the carbon fiber rod to be the same height. This way when the servo connected to the first bar turns 1 degree, the third bar turns at the same rate.

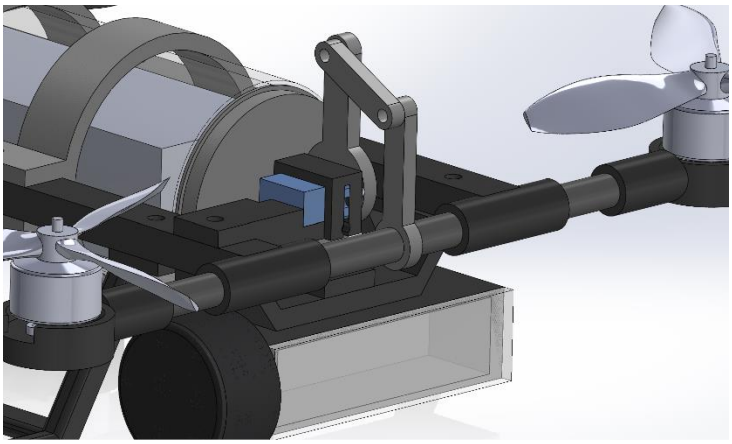

Figure 31: Three bar linkage in Quadcopter Mode.

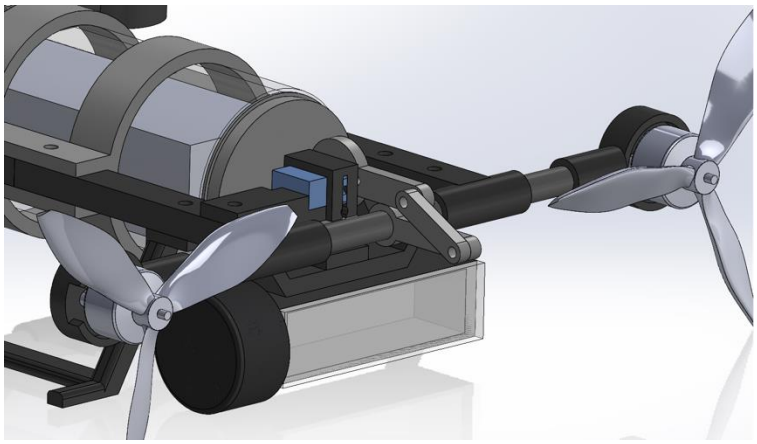

Figure 32: Three bar linkage in Quadplane Mode.

The tiltrotor design 2 proved much more effective and reliable than the previous design. By joining the 3 bars together, it eliminated the risk of failure due to slippage seen in the gears. With this design, the largest cause of failure would now be due to a malfunction within the servo.

3.4.7 Waterproof Servo

One challenge our team faced was designing a system that minimized the risk of the servo failing while being submerged in the water. In our design, we attached a servo motor to the front of our quad rotor leaving it fully exposed to its surroundings. This meant that when the quadrotor transitioned from quadcopter to quadplane mode, it would need to do so with no effect from the water. Through our research, the team came up with two ideas. The first option would be to buy a commercial waterproof servo which the team quickly realized would not be a viable option. Most small commercially advertised waterproof servos are not waterproof, rather water resistant. They can be splashed by water and still function properly but are not able to be fully submerged. When they are fully submerged, the pressure differential causes water to leak into the body of the servo where the hardware is held. The few that claim to be waterproof are expensive and were out of the team's budget, especially since we could not confirm they would be any more successful. This meant that the team's only option would be to use a regular servo and modify it to keep water from entering the servo.

Through our research, we found different techniques to waterproof a servo from submarine hobbyist. The two primary methods the team used were from RCSubGuy and Blue Dot ROV on YouTube. For their RC submarines they modify the servos by filling them with mineral or olive oil and sealing the edges. When the servos are filled with an incompressible fluid like mineral oil, the pressure differential in the servo is eliminated. They also sealed the cracks around the edges with an adhesive and sprayed a layer of flex seal. Lastly, they put a fitted O-ring around the gear that is compressed down with the servo horn sealing the opening on top. We had followed the same procedure using mineral oil, 5200 Marine Adhesive and flex seal. Through our tests, we found that this method does temporarily waterproof the servos. The waterproof servos we made survived many tests before they broke. Although this method did not work perfectly, it extended the life of our servos and reduced the probability of the servo failing per flight [13] [14].

3.5 Hydrostatics Analysis

In our examination of the hydrostatics for our AUV, we undertook a comprehensive approach to optimizing weight distribution across its framework. This was done with the goal of ensuring that the AUV's center of mass remains vertically aligned beneath its center of buoyancy, as illustrated in Figure 33.We acknowledge that any deviation where the center of mass is above the center of buoyancy would predispose the AUV to instability, resulting in unintended flipping when fully submerged, as depicted in Figure 34.

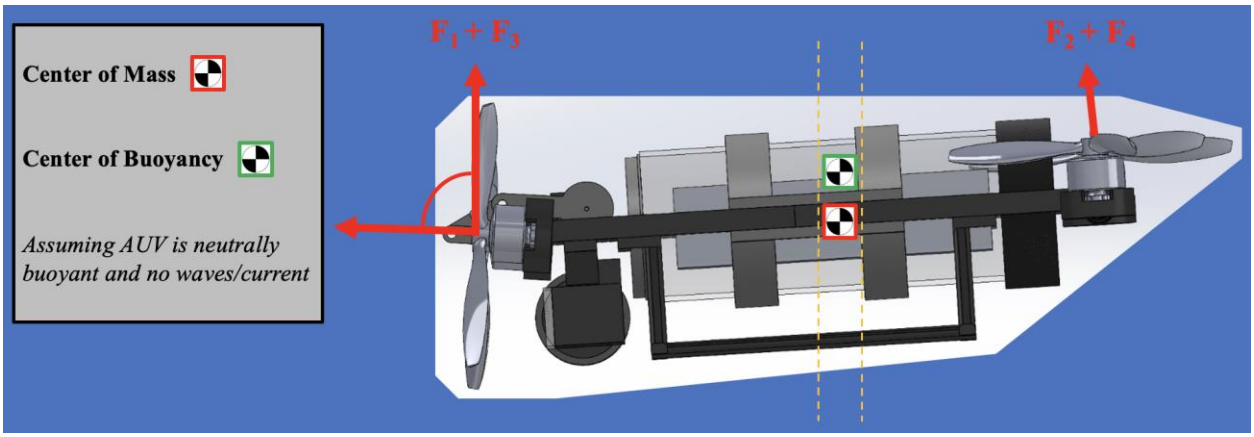

Figure 33: Stable Location for Center of Buoyancy.

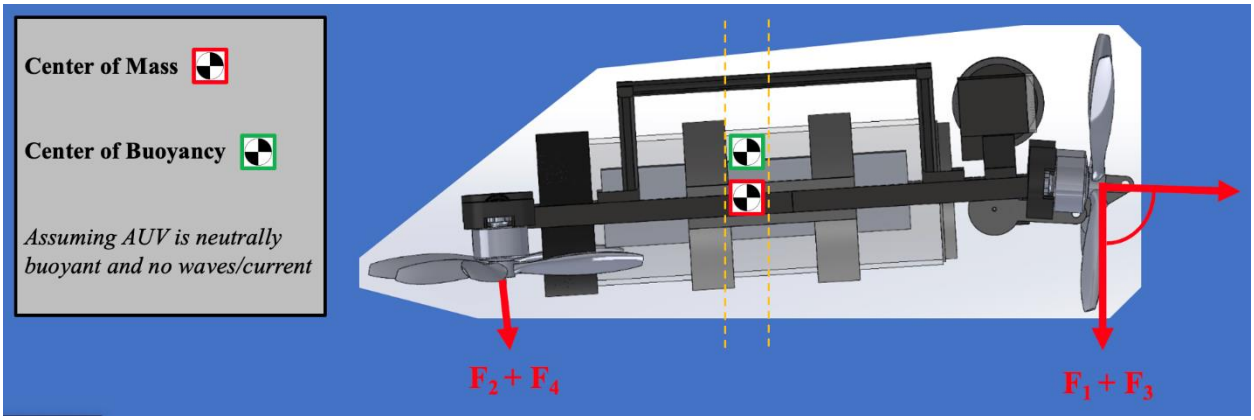

Figure 34: Unstable Location for Center of Buoyancy.

This is crucial for our AUV so that it can operate underwater and achieve the mission objective. For simplicity's sake, we assumed that the AUV is neutrally buoyant, meaning that the AUV does not sink or float in water. This allowed us to simplify our equations of motion. We also assumed there were no waves and/or current affecting the AUV since the underwater locomotion was taking place in an in-door pool setting.

3.6 Propulsive Analysis

Due to the complex nature of the requirements for the AUV's performance, there is a significant need for detailed analysis of the capabilities of any proposed propulsion system. The capabilities of said system in aerial flight and underwater must be balanced to ensure it can adequately perform in both environments. Based on some preliminary assumptions and observations, some basic guidelines for what would be required can be created. However, a more in-depth computational analysis of the efficiency of propulsion elements in the relevant environments was required.

3.6.1 Propeller Selection

Based on the project's design requirements, it was determined early on that the propulsion system would need to be far more efficient in aerial flight than underwater. This meant that the design of the propellers would need to be primarily intended for use in air, with some considerations made and analysis done to simultaneously maximize its efficiency and performance in an aquatic environment.

One of the main differences between the properties of air and water for this application is the fluid's density. This traditionally influences the differences in the design of propellers intended for use in air and water. Propellers intended for use in air typically have much longer blade lengths, far lower surface area to blade length ratios (i.e., narrower blades) and operate at much higher speeds than those designed for water. Having a greater propeller diameter in water (longer blade length) has a far greater effect on the torque required to drive said propeller. At the same time, propeller diameter and surface area have a great effect on efficiency and thrust output, and decreasing the diameter of the propellers to enhance aquatic performance could have a notable impact on the aerial effectiveness. As such, different ways of maximizing propeller surface area while minimizing blade length must be considered to maintain the necessary thrust output. The recommended diameter of propellers for the motors chosen are around eight inches and above; however, a slightly smaller propeller diameter of 7 inches with a pitch of 3.5 inches was initially determined to be preferable due to the considerations listed above. To lessen the losses in thrust output and efficiency due to this decision, three bladed propellers were utilized to increase the surface area without increasing diameter.

It was determined based on early flight tests that the power supply and battery life presented an unforeseen challenge for the design. It was originally intended for the motors to run at high RPM (around 18000) for flight in an aerial environment, this was determined based on data gathered during our efficiency analysis in 3.6.2 Aerial and Underwater Efficiency Analysis. With the initially selected motors and battery it would not be possible to achieve those speeds. Furthermore, such conditions would negatively impact possible battery life and, by extension, limit flight duration. As a solution to these problems, it was decided that slightly larger propellers of an 8-inch diameter and a slightly more aggressive pitch of 4 inches should be utilized to decrease the motor speeds necessary for flight.

3.6.2 Aerial and Underwater Efficiency Analysis

Because the propellers used are designed for use in air, detailed pre-existing information on their performance in an aquatic environment is lacking. To determine the specific effect of details such as blade shape and pitch in such an environment, computational analysis of various propeller designs was carried out using ANSYS software. The FLUENT module of ANSYS was used to conduct fluidic simulations of the operation of these propeller designs in both air and water. To start with, designs with blade pitches of 35, 40 and 56 degrees with similar blade shapes were considered. This was eventually expanded to examine the impact of specific blade profiles on performance, with the blade geometry tweaked to more closely match the shape of the exact propellers being used. Scaled propeller models were also used to analyze the impact of different diameters, and by extension, blade lengths on performance. The actual simulation model utilized was a K-Epsilon type, with the propeller blade mesh placed in a rotating cylindrical region. This was bounded by a region of fluid which was initially at rest as shown in Figure 35: Propeller simulation/region setup (8040 shown). below. The simulations were run for

a sufficient amount of time for the flow to reach a steady state, after which thrust and torque readings were averaged over a range of timestamps.

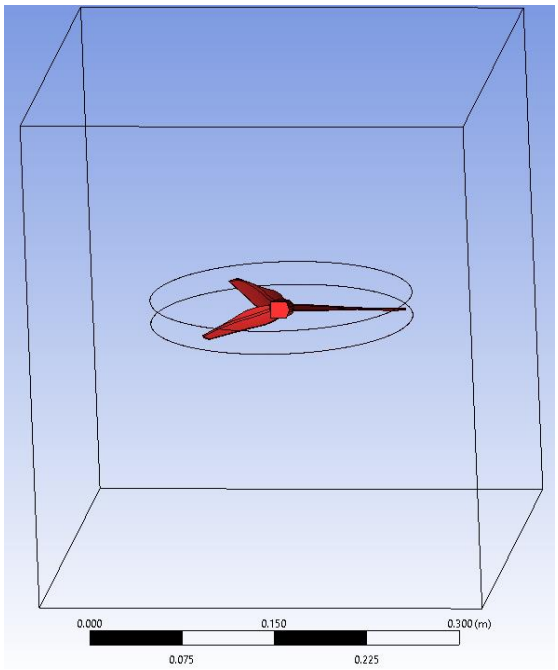

Figure 35: Propeller simulation/region setup (8040 shown).

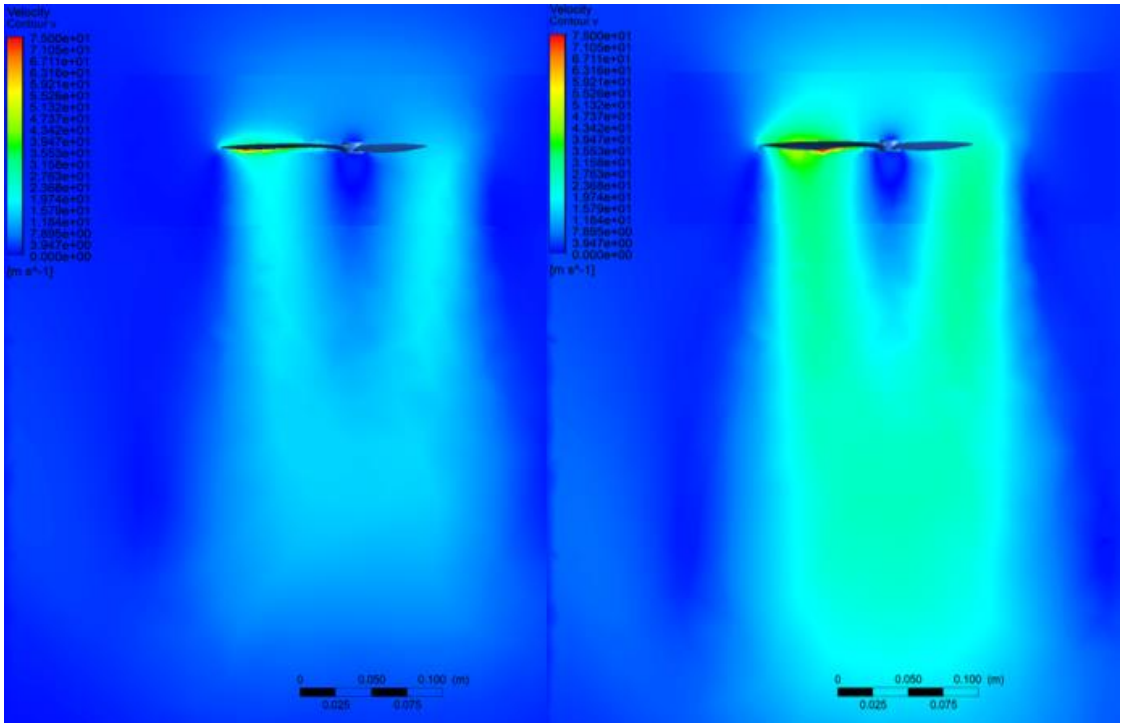

Figure 36: Steady-state flow in air for 7056 propeller at 9000 RPM (left) and 16000 RPM (right).

The resulting data from said simulations was then used to plot the estimated performance of the different propeller profiles at all rotation speeds. For example, the plots generated for 8040 propellers of a similar profile to the ones ultimately used can be seen in Figure 37 below. Functions relating thrust and torque values to rotation speed were also developed from these plots. These functions were then used with the derived vehicle dynamics to simulate different maneuvers and the control inputs needed for the AUV to perform them.

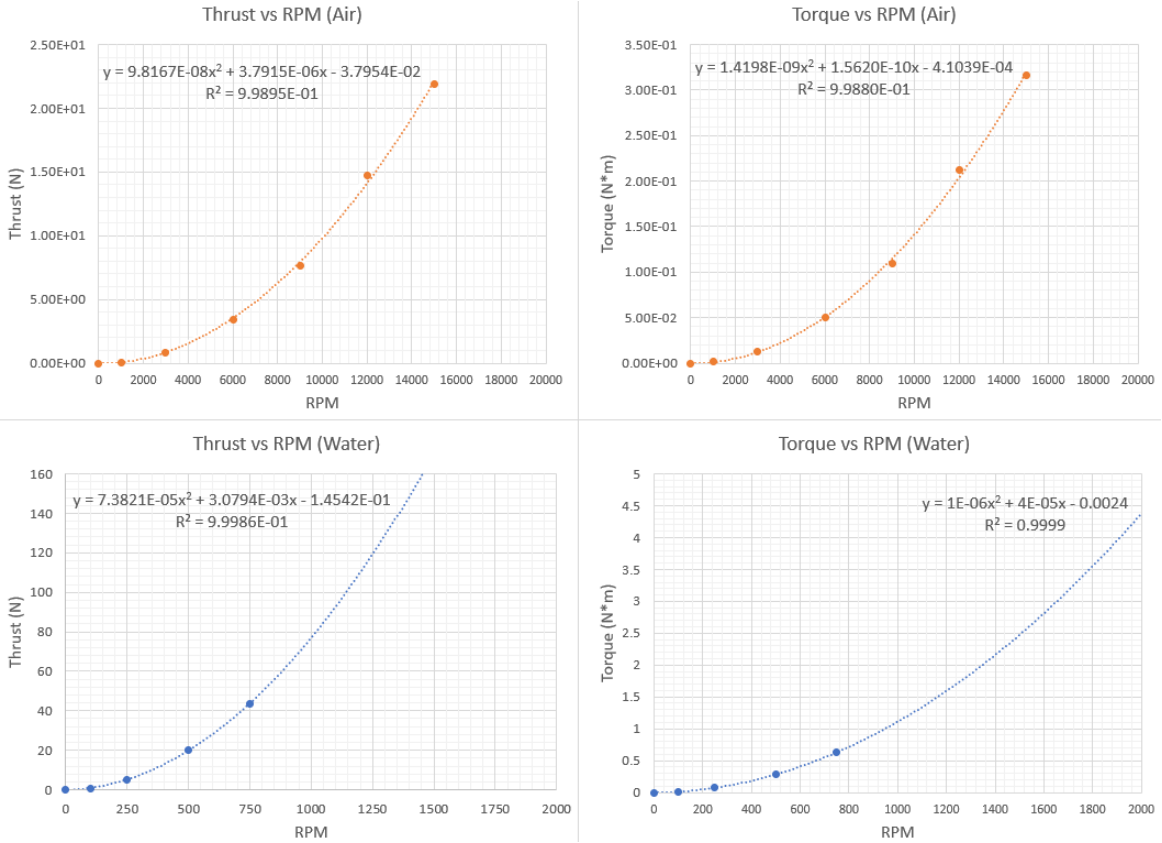

Figure 37: Generated performance plot/functions for 8040 propellers.

4 Results

4.1 Summary

Through the extensive research and testing discussed, the following results were achieved. The vehicle proved to be capable of effective locomotion both underwater and in air in initial tests in both environments, proving the effectiveness of developed tiltrotor concept. The AUV also demonstrated the capability to transfer between air and water in repeated testing. The final test of the AUV was to complete the mission described in the project description, take off from the pool deck, transition into the water, and travel one full pool length underwater and then fly back to the starting point. The AUV was able to complete this mission using manual controls, as unfortunately, the underwater autonomy had not been completed in the time of final testing.

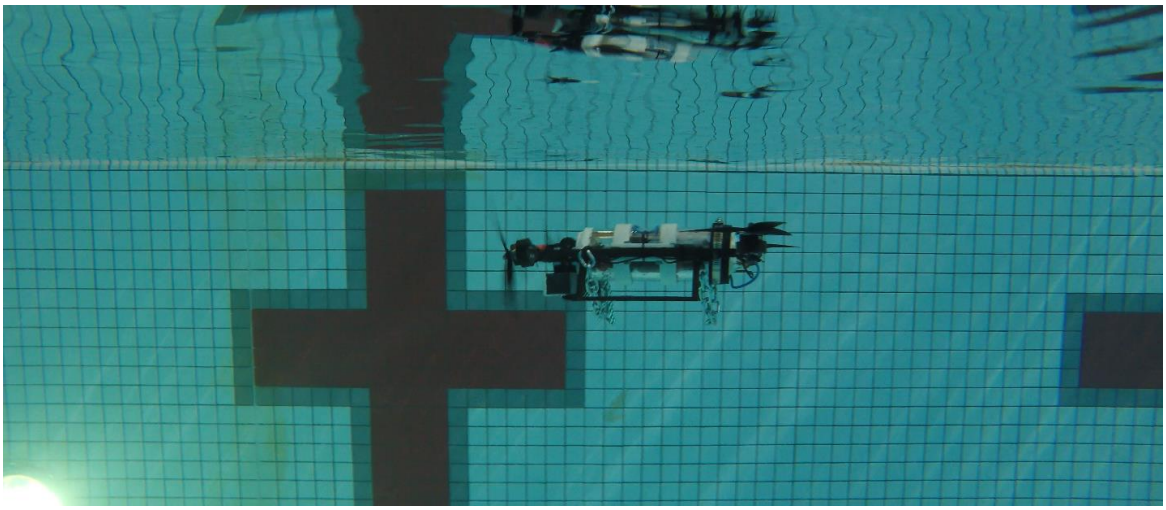

Figure 38: AUV Locomotion Fully Submerged.

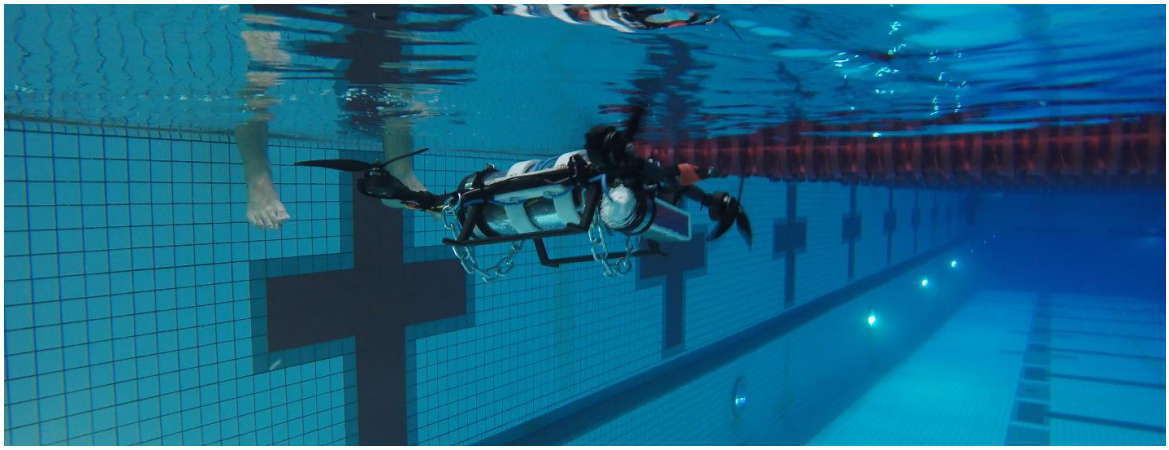

Figure 39: AUV Fully Submerged with Front Arm Fixed.

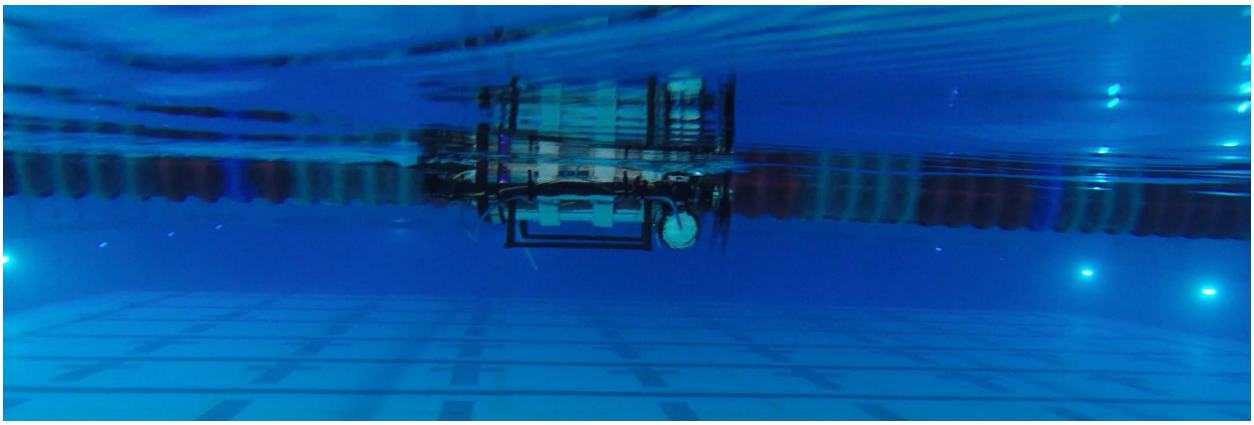

Figure 40: AUV Travelling Semi-Submerged.

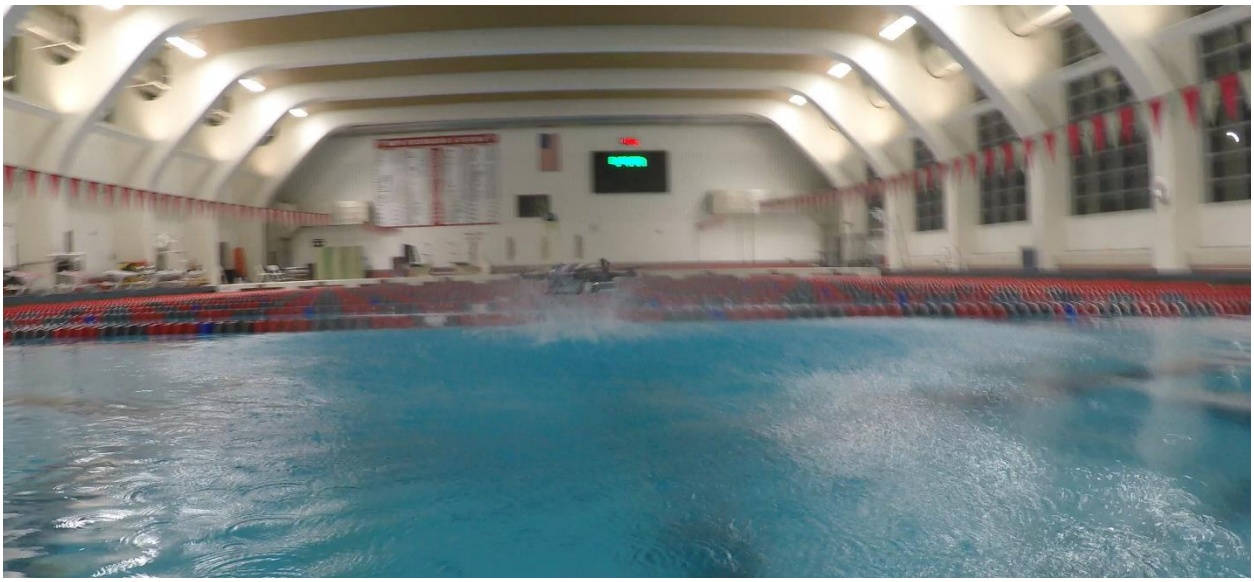

Figure 41: AUV Water to Air Transition.

The team determined that the best option for waterproofing was to utilize commercially available components for watertight enclosures as opposed to using 3D printed parts as was done for much of the other structural components of the vehicle. The team also conducted in-depth analysis of the hydrostatics and hydrodynamics of the AUV in order to better understand its behavior underwater. Further progress was also made on developing the vehicles autonomous control and navigation capability, autonomous aerial flight was achieved but underwater autonomy was not completed by the time of testing. Testing was done on the viability of methods of communication with the vehicle while submerged. Limitations in the ArduPlane software were identified and solutions or workarounds for some of these were examined. Insufficiencies with the Pixhawk flight controllers were also determined. Lastly, the team did extensive research into methods of waterproofing servos for the actuation of the tilt rotor mechanism. The research and work detailed above should prove to be a strong foundation for future work on similar projects.

4.2 Conclusions

The primary objective of this project was to design, build, and test an amphibious AUV capable of seamless transition between both aerial and underwater flight and navigation in a GPS denied environment. The developed design has proven through repeated and varied testing to be a viable design for fulfilling the aforementioned criteria. It effectively solves many of the problems faced by the previous MQP project group with their design. The tilt-rotor concept proved to be a viable replacement for the active ballast system of the previous design and allowed for improved underwater mobility. The AUV also proved capable of both air-to-water and water-to-air transitions during testing. Additionally, the usage of primarily “purpose built” commercially available components for watertight enclosures avoided the waterproofing issues experienced by the previous group. Finally, the stability exhibited by the vehicle during testing in both air and water supports the validity of our Hydrostatic analysis. Based on the presented information and test results, the designed AUV represents a viable solution to the project's central problem and objective.

4.3 Recommendations for Future Work

The team has a few recommendations for future projects undertaking similar objectives based on the research and development completed. From the team’s progress building off the previous MQP project, the desired mission is attainable by focusing on a few key areas and iterating our design.

The first recommendation is to use a lower frequency radio transmitter to operate the AUV underwater. The frequency our transmitter used was 2.4 GHz which had trouble communicating underwater and lost signal after the craft was submersed in a depth of 18 inches. Due to this limitation, we could not test our AUV any deeper because if a malfunction occurred while traversing the water autonomously, we could not switch to manual mode. This can be avoided by using a radio operating at a lower frequency like 75 MHz.

The second recommendation is to spend time editing the source code of ArduPlane to allow for a small amount more customizability for autonomous flight. There are two settings in ArduPlane that are not able to be changed with surface level parameters and commands, these two settings are the only reason we were not able to fly the full aerial to underwater mission. The first thing that needs to be changed is the default frame configuration for autonomous flight using a quad plane. When autonomous flight is triggered in a quad plane frame type the autopilot will default to using the plane frame configure for movement between waypoints, meaning that after takeoff vertical the AUV would dive out of the air after switching the propellers forward. There is another potential workaround for editing a parameter which indicates how far from a waypoint the AUV needs to be for VTOL flight, but we did not have enough time to thoroughly test this option. We would recommend just editing the actual autopilot code to allow for the frame configuration to be chosen when entering autonomous flight. The second setting that needs to be changed is the Q_ASSIST feature, which allows for the two rear vertical propellers to assist the AUV in rolling and pitching. For submerged flight this feature is activated prematurely due to the Q_ASSIST_SPEED, as the autopilot believes the plane is stalling when it is not moving causing it to send overly strong impulses to the motors to account for this. If Q_ASSIST_SPEED

could be disabled, and these motors only used for rolling and pitching the AUV would be much more stable while traversing a submerged domain.

Another recommendation for the next MQP team to swap flight controllers from the original Pixhawk to another flight controller with more robust IMUs. The reason for this is because the Pixhawk was having trouble maintaining accurate reading as it is a legacy platform with a low to mid-level sensor suite. For the new iteration, a newer flight controller with robust IMU's including multiple sets for redundancy. In addition to this, finding a better way to validate the altitude in both the water and air would be smart. With the flight controller enclosed in a pressure sealed container, the barometer is neglected, meaning the AUV is relying on just the tracking camera for altitude. Unfortunately, the tracking camera is not very reliable for altitude when facing forwards, meaning we had altitude variations when running autonomous missions.

Our last recommendation is to explore and test other options for a more reliable long-term waterproof servo. We decided to buy and modify many cheap servos rather than invest a large portion of the budget into one reliable waterproof servo. As a team we spent a significant amount of time modifying the servos which extended their lifespan underwater but, was a band aid and not a long-term solution. Having a dependable servo would have allowed us to attempt more controlled and autonomous tests in the pool.

4.4 Broader Impact

The applications of this project are wide reaching. From civilian to military there are many places where an autonomous AUV could be applied. The AUV could be launched from a boat and submerged to check underwater fiber optics or to monitor underwater repairs on oil rigs. Along with these applications, the project also provided further understanding of the design goals. The design of the tilt-rotor locomotion, techniques developed in waterproofing and rapid prototyping of the frame, analysis of the propulsion system and AUV capabilities, and programming of the autonomous flight all can be used in future projects to aid in design development, especially another iteration of this project.

References

[1] J. Guilmartin, "Unmanned Aerial Vehicles," in *Britannica Encyclopedia*, 2023.

[2] S. Norouzi Ghazbi, Y. Aghli, M. Alimohammadi and A. A. Akbari, "Quadrotors Unmanned Aerial Vehicles: A Review," *International Jopurnal on Smart Sensing and Intelligent Systems*, vol. 9, no. 1, 2016.

[3] S. Bin Nazarudeen and J. Liscouet, "State-Of-The-Art And Directions For The Conceptual Design Of Safety-Critical Unmanned And Autonomous Aerial Vehicles," *2021 IEEE INternational Conference on Autonomous Systems (ICAS)*, 2021.

[4] P. L. J. Drews Jr., A. Alves Neto and M. F. M. Campos, "Hybrid Unmanned Aerial Vehicles: Modeling and Simulation," *IEEE*.

[5] D. Israel, "The Daily Targum," Targum Publishing Company, 2024. [Online]. Available: https://dailytargum.com/article/2017/09/rutgers-professor-creates-drone-capable-of-both-flying-and-swimming.

[6] D. K. Craig, *Quadrotor Equations of Motion and Control KCC FInal 4 2023 Video*, 2023.

[7] M. Narasimhappa, A. D. Mahindrakar, V. C. Guizilini, M. H. Terra and S. L. Sabat, "MEMS-Based IMU Drift Minimization: Sage Husa Adaptive Robust Kalman Filtering," *IEEE Sensors Journal*, vol. 20, no. 1, pp. 250-260, 2019.

[8] Adafruit, "Raspberry Pi 3 - Model B - ARMv8 with 1G RAM," Adafruit, [Online]. Available: https://www.adafruit.com/product/3055.

[9] ArduPilot, "Intel RealSense T265," ArduPilot Dev Team, 2024. [Online]. Available: https://ardupilot.org/copter/docs/common-vio-tracking-camera.html.

[10] ArduPilot, "Extended Kalman Filter (EKF)," ArduPilot Dev Team, 2024. [Online]. Available: https://ardupilot.org/copter/docs/common-apm-navigation-extended-kalman-filter-overview.html.

[11] BlueRobotics, "BlueRobotics - Watertight Enclosure," Blue Robotics Inc., 2024. [Online]. Available: https://bluerobotics.com/store/watertight-enclosures/wte-vp/#tube.

[12] M. Beskid, R. Brunelle, C. Carrignan, R. Devlin, T. Patel and K. Sarfo, "Design and Testing of an Amphibious AUV," Worcester Polytechnic Institute, Worcester, MA, 2023.

[13] RCSubGuy, *How to make a true waterproof servo.*, 2020.

[14] B. D. ROV, *Waterproofing a Servo Motor for RC Submarine Dives*, 2021.

Appendix A – Aerial Dynamics Derivation

Physical Model Simplifying Assumptions

1. The AUV is treated as a rigid body.
2. The motors and propellers provide perfect thrust and control.
3. Aerodynamic effects and wind are neglected.
4. External disturbances are ignored.

Definitions

Linear Velocities in AUV Body-fixed Frame

$$\boldsymbol{v}^b = \begin{bmatrix} u \\ v \\ w \end{bmatrix}^b = \begin{bmatrix} \text{longitudinal velocity} \\ \text{lateral velocity} \\ \text{vertical velocity} \end{bmatrix}$$

Angular Velocities in AUV Body-fixed Frame

$$\boldsymbol{\omega} = \begin{bmatrix} p \\ q \\ r \end{bmatrix} = \begin{bmatrix} \text{roll rate} \\ \text{pitch rate} \\ \text{yaw rate} \end{bmatrix}$$

Forces acting on AUV

$$\boldsymbol{F} = \begin{bmatrix} F_x \\ F_y \\ F_z \end{bmatrix} = \begin{bmatrix} \text{force in the body} - \text{fixed x direction} \\ \text{force in the body} - \text{fixed y direction} \\ \text{force in the body} - \text{fixed z direction} \end{bmatrix}$$

Moments acting on AUV

$$\boldsymbol{M} = \begin{bmatrix} L \\ M \\ N \end{bmatrix} = \begin{bmatrix} \text{moment about the body} - \text{fixed x axis} \\ \text{moment about the body} - \text{fixed y axis} \\ \text{moment about the body} - \text{fixed z axis} \end{bmatrix}$$

Euler Angles

$$\boldsymbol{\Phi} = \begin{bmatrix} \phi \\ \theta \\ \psi \end{bmatrix} = \begin{bmatrix} \text{roll angle} \\ \text{pitch angle} \\ \text{yaw angle} \end{bmatrix}$$

Absolute Position in Inertial Navigation Frame

$$\boldsymbol{S} = \begin{bmatrix} X \\ Y \\ H \end{bmatrix} = \begin{bmatrix} \text{longitudinal position} \\ \text{lateral position} \\ \text{height} \end{bmatrix}$$

Translational Motion

Newton's Second Law

$$\boldsymbol{F} = \frac{d\boldsymbol{p}}{dt} = m\frac{d\boldsymbol{v}}{dt} = m\boldsymbol{a}$$

Velocity in Body-fixed Frame

$$\boldsymbol{v}^b = \begin{bmatrix} u \\ v \\ w \end{bmatrix}^b = u\hat{x}_b + v\hat{y}_b + w\hat{z}_b$$

Acceleration in Body-fixed Frame

$$\left(\frac{d\boldsymbol{v}^b}{dt}\right)_{inertial} = \left(\frac{du}{dt}\hat{x}_b + \frac{dv}{dt}\hat{y}_b + \frac{dw}{dt}\hat{z}_b\right) + \left(u\frac{d\hat{x}_b}{dt} + v\frac{d\hat{y}_b}{dt} + w\frac{d\hat{z}_b}{dt}\right)$$

$$\dot{\boldsymbol{v}}_n^b = \dot{\boldsymbol{v}}^b + \dot{\boldsymbol{\omega}}_n^b \times \boldsymbol{v}^b$$

$$\dot{\boldsymbol{v}}_n^b = \begin{bmatrix} \dot{u} \\ \dot{v} \\ \dot{w} \end{bmatrix} + \begin{bmatrix} 0 & -r & q \\ r & 0 & -p \\ -q & p & 0 \end{bmatrix} \begin{bmatrix} u \\ v \\ w \end{bmatrix} = \begin{bmatrix} \dot{u} + q\,w - r\,v \\ \dot{v} + r\,u - p\,w \\ \dot{w} + p\,v - q\,u \end{bmatrix}$$

Force Exerted by Propeller Thrust

$$\boldsymbol{F}_{prop} = \begin{bmatrix} F_x \\ F_y \\ F_z \end{bmatrix} = \begin{bmatrix} 0 \\ 0 \\ F_1 + F_2 + F_3 + F_4 \end{bmatrix}$$

Gravitational Force in Inertial and Body-fixed Frame

$$\boldsymbol{F}_{grav}^{n} = \begin{bmatrix} 0 \\ 0 \\ mg \end{bmatrix} \rightarrow \boldsymbol{F}_{grav}^{b} = \begin{bmatrix} m\ g\ s(\theta) \\ -m\ g\ s(\phi)\ \mathrm{c}(\theta) \\ -m\ g\ c(\phi)\ \mathrm{c}(\theta) \end{bmatrix}$$

$$\boldsymbol{F}_{prop} + \boldsymbol{F}_{grav} = m\dot{\boldsymbol{v}}_{n}^{b}$$

$$\begin{bmatrix} m\ g\ s(\theta) \\ -m\ g\ s(\phi)\ \mathrm{c}(\theta) \\ F_1 + F_2 + F_3 + F_4 - m\ g\ c(\phi)\ \mathrm{c}(\theta) \end{bmatrix} = m \begin{bmatrix} \dot{u} + q\ w - r\ v \\ \dot{v} + r\ u - p\ w \\ \dot{w} + p\ v - q\ u \end{bmatrix}$$

Equations of Motion (Linear Acceleration)

$$\dot{u} = g\ s(\theta) - q\ w + r\ v$$

$$\dot{v} = -g\ s(\phi)\ \mathrm{c}(\theta) - r\ u + p\ w$$

$$\dot{w} = \frac{1}{m}(F_1 + F_2 + F_3 + F_4) - g\ c(\phi)\ \mathrm{c}(\theta) - p\ v + q\ u$$

Rotational Motion

Moment Angular Velocity Relationship

$$M = \frac{d\boldsymbol{H}}{dt} = I\frac{d\boldsymbol{\omega}}{dt} = I\boldsymbol{\Omega}$$

Chain Rule Derivation

$$\boldsymbol{M} = I\frac{d\boldsymbol{\omega}}{dt} \rightarrow \boldsymbol{M} = I\dot{\boldsymbol{\omega}}_n^b + \boldsymbol{\omega}_n^b \times I\boldsymbol{\omega}_n^b$$

Moment of Inertia Matrix

$$I = \begin{bmatrix} I_{xx} & -I_{xy} & -I_{xz} \\ -I_{xy} & I_{yy} & -I_{yz} \\ -I_{xz} & -I_{yz} & I_{zz} \end{bmatrix}$$

$$\boldsymbol{M} = I\dot{\boldsymbol{\omega}}_n^b + \boldsymbol{\omega}_n^b \times I\boldsymbol{\omega}_n^b$$

$$\begin{bmatrix} L \\ M \\ N \end{bmatrix} = \begin{bmatrix} I_{xx} & -I_{xy} & -I_{xz} \\ -I_{xy} & I_{yy} & -I_{yz} \\ -I_{xz} & -I_{yz} & I_{zz} \end{bmatrix} \begin{bmatrix} \dot{p} \\ \dot{q} \\ \dot{r} \end{bmatrix} + \begin{bmatrix} 0 & -r & q \\ r & 0 & -p \\ -q & p & 0 \end{bmatrix} \begin{bmatrix} I_{xx} & -I_{xy} & -I_{xz} \\ -I_{xy} & I_{yy} & -I_{yz} \\ -I_{xz} & -I_{yz} & I_{zz} \end{bmatrix} \begin{bmatrix} p \\ q \\ r \end{bmatrix}$$

$$\begin{bmatrix} L \\ M \\ N \end{bmatrix} = \begin{bmatrix} I_{xx}\dot{p} - I_{xy}\dot{q} - I_{xz}\dot{r} - p\left(I_{xz}q - I_{xy}r\right) - q\left(I_{yz}q + I_{yy}r\right) + r\left(I_{zz}q + I_{yz}r\right) \\ I_{yy}\dot{q} - I_{xy}\dot{p} - I_{yz}\dot{r} + p(I_{xz}p + I_{xx}r) + q\left(I_{yz}p - I_{xy}r\right) - r(I_{zz}p + I_{xz}r) \\ I_{zz}\dot{r} - I_{yz}\dot{q} - I_{xz}\dot{p} - p\left(I_{xy}q + I_{xx}q\right) + q\left(I_{yy}p + I_{xy}q\right) - r\left(I_{yz}p - I_{xz}q\right) \end{bmatrix}$$

From our one-to-one SolidWorks model, the computed moment of inertia matrix came out to:

$$I = \begin{bmatrix} 0.014051 & -0.001120 & -0.000984 \\ -0.001120 & 0.028973 & 0.000319 \\ -0.000984 & 0.000319 & 0.040233 \end{bmatrix} kg * m^2$$

Since the off-diagonal elements of the moment of inertia matrix are two to even three orders of magnitude smaller than the diagonal elements we went with the assumption of our moment of inertia matrix being:

$$I = \begin{bmatrix} Ixx & 0 & 0 \\ 0 & Iyy & 0 \\ 0 & 0 & Izz \end{bmatrix}$$

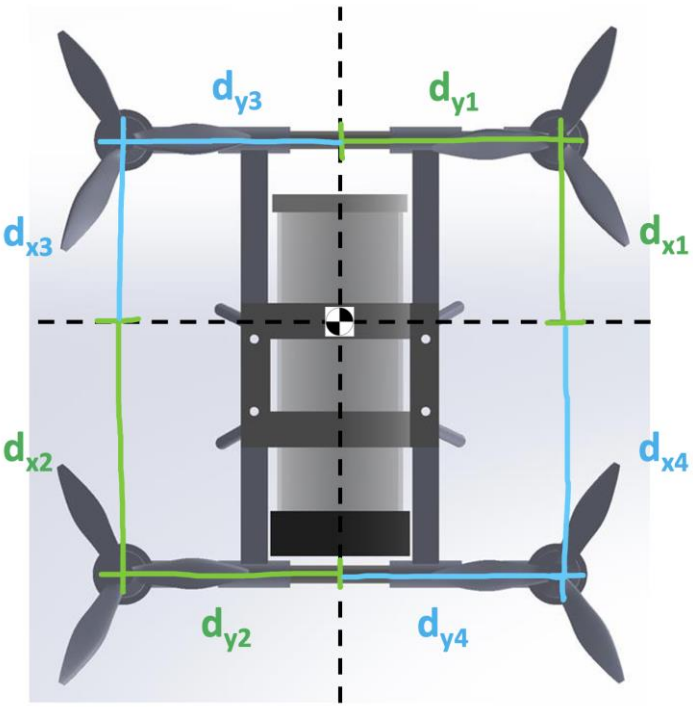

Figure 42: X and Y displacement from Body-fixed Origin (AUV CoM).

$$L = -F_1 d_{1y} + F_2 d_{2y} + F_3 d_{3y} - F_4 d_{4y}$$

$$M = -F_1 d_{1x} + F_2 d_{2x} - F_3 d_{3x} + F_4 d_{4x}$$

$$N = T_1 + T_2 - T_3 - T_4$$

Equations of Motion (Angular Acceleration)

$$\dot{p} = \frac{\left(L + I_{xy}\dot{q} + I_{xz}\dot{r} + p\left(I_{xz}q - I_{xy}r\right) + q\left(I_{yz}q + I_{yy}r\right) - r\left(I_{zz}q + I_{yz}r\right)\right)}{I_{xx}}$$

$$\dot{q} = \frac{\left(M + I_{xy}\dot{p} + I_{yz}\dot{r} - p(I_{xz}p + I_{xx}r) - q\left(I_{yz}p - I_{xy}r\right) + r(I_{zz}p + I_{xz}r)\right)}{I_{yy}}$$

$$\dot{r} = \frac{\left(N + I_{xz}\dot{p} + I_{yz}\dot{q} + p\left(I_{xy}p + I_{xx}q\right) - q\left(I_{yy}p + I_{xy}q\right) + r\left(I_{yz}p - I_{xz}q\right)\right)}{I_{zz}}$$

However, with the assumption of our moment of inertia matrix being:

$$I = \begin{bmatrix} Ixx & 0 & 0 \\ 0 & Iyy & 0 \\ 0 & 0 & Izz \end{bmatrix}$$

The angular acceleration equations simplify to:

$$\dot{p} = \frac{L}{I_{xx}} - \left(\frac{I_{yy} - I_{zz}}{I_{xx}}\right) q\, r$$

$$\dot{q} = \frac{M}{I_{yy}} - \left(\frac{I_{zz} - I_{xx}}{I_{yy}}\right) p\, r$$

$$\dot{r} = \frac{N}{I_{zz}} - \left(\frac{I_{xx} - I_{yy}}{I_{zz}}\right) p\, q$$

To extract information about the AUV in relation to the body-fixed frame from the inertial navigation frame, a series of intermediate frames are employed. This process involves the establishment of two intermediary frames: R1, which arises from a yaw rotation of the inertial navigation frame, and R2, which emerges through a subsequent pitch rotation of R1. Lastly, R3 is derived by applying a roll rotation to R2, resulting in the body-fixed reference frame. These intermediate frames serve as critical components in deriving the equations of motion for the AUV. They are essential for seamlessly transitioning from the inertial navigation frame to the body-fixed reference frame, enabling accurate modeling and analysis of the AUV's dynamics and behavior.

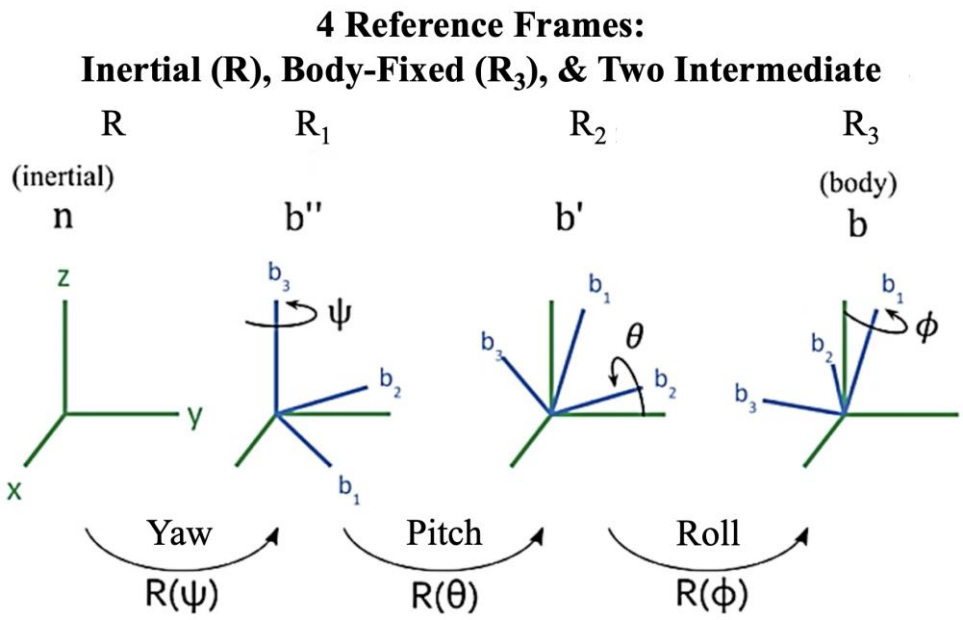

Figure 43. Reference Frames used for Coordinate Transformation [6].

Equations of Motion in Inertial Navigation Frame

Linear Velocity Rotation Matrix (Body-fixed to Inertial Reference Frame)

$$R_b^n = \begin{bmatrix} \mathrm{c}(\theta)\,\mathrm{c}(\phi) & \mathrm{s}(\phi)\,\mathrm{s}(\theta)\,\mathrm{c}(\psi) - \mathrm{c}(\phi)\,\mathrm{s}(\psi) & \mathrm{s}(\phi)\,\mathrm{s}(\psi) + \mathrm{c}(\phi)\,\mathrm{s}(\theta)\,\mathrm{c}(\psi) \\ \mathrm{c}(\theta)\,\mathrm{s}(\psi) & \mathrm{c}(\phi)\,\mathrm{c}(\psi) + \mathrm{s}(\phi)\,\mathrm{s}(\theta)\,\mathrm{s}(\psi) & \mathrm{c}(\phi)\,\mathrm{s}(\theta)\,\mathrm{s}(\psi) - \mathrm{s}(\phi)\,\mathrm{c}(\psi) \\ -\mathrm{s}(\theta) & \mathrm{s}(\phi)\,\mathrm{c}(\theta) & \mathrm{c}(\phi)\,\mathrm{c}(\theta) \end{bmatrix}$$

Linear Velocity

$$\dot{X} = (\mathrm{c}(\theta)\,\mathrm{c}(\phi))u + (-\mathrm{c}(\phi)\,\mathrm{s}(\psi) + \mathrm{s}(\phi)\,\mathrm{s}(\theta)\,\mathrm{c}(\psi))v + (\mathrm{s}(\phi)\,\mathrm{s}(\psi) + \mathrm{c}(\phi)\,\mathrm{s}(\theta)\,\mathrm{c}(\psi))w$$

$$\dot{Y} = (\mathrm{c}(\theta)\,\mathrm{s}(\psi))u + (\mathrm{c}(\phi)\,\mathrm{c}(\psi) + \mathrm{s}(\phi)\,\mathrm{s}(\theta)\,\mathrm{s}(\psi))v + (-\mathrm{s}(\phi)\,\mathrm{c}(\psi) + \mathrm{c}(\phi)\,\mathrm{s}(\theta)\,\mathrm{s}(\psi))w$$

$$\dot{H} = (-\mathrm{s}(\theta))u + (\mathrm{s}(\phi)\,\mathrm{c}(\theta))v + (\mathrm{c}(\phi)\,\mathrm{c}(\theta))w$$

Angular Velocity Rotation Matrix (Body-fixed to Inertial Reference Frame)

$$R_b^n = \begin{bmatrix} 1 & \sin(\phi)\tan(\theta) & \cos(\phi)\tan(\theta) \\ 0 & \cos(\phi) & -\sin(\phi) \\ 0 & \sin(\phi)\sec(\theta) & \cos(\phi)\sec(\theta) \end{bmatrix}$$

Euler Angles Rate of Change

$$\dot{\phi} = p + q(\sin(\phi)\tan(\theta)) + r(\cos(\phi)\tan(\theta))$$

$$\dot{\theta} = q(\cos(\phi)) - r(\sin(\phi))$$

$$\dot{\psi} = q(\sin(\phi)\sec(\theta)) + r(\cos(\phi)\sec(\theta))$$

The use of different rotation matrices for converting body-fixed linear velocities to inertial frame linear velocities and body-fixed angular velocities to inertial frame angular velocities is rooted in the fundamental distinction between these two types of motion and their respective representations in the context of rigid body dynamics. Linear velocities pertain to translational motion, describing how an object moves through space, while angular velocities relate to rotational motion, signifying how an object rotates about its center of mass. Linear velocities are represented as 3D vectors, and to convert them to the inertial frame, a standard 3x3 rotation matrix is employed. This matrix accommodates changes in the object's orientation when transitioning from the body-fixed frame to the inertial frame, ensuring that the linear velocities are correctly transformed. On the other hand, angular velocities are also represented as 3D vectors but undergo transformation using a skew-symmetric matrix due to their unique properties associated with vector cross products and the behavior of angular velocities when transitioning between frames. Consequently, the use of distinct rotation matrices for linear and angular velocities is necessitated by the inherent disparities in these two types of motion and the mathematical properties governing their conversions between frames.

Appendix B - Aerial Dynamics Validation Results

Table 2: AUV Hovering Motor Data for a Mass of 2.72 kg (0.45 kg of payload).

Hover			
Motor	**RPM**	**Thrust [N]**	**Torque [N-m]**
1	8249	6.6732	0.0962
2	8249	6.6732	0.0962
3	8249	6.6732	0.0962
4	8249	6.6732	0.0962

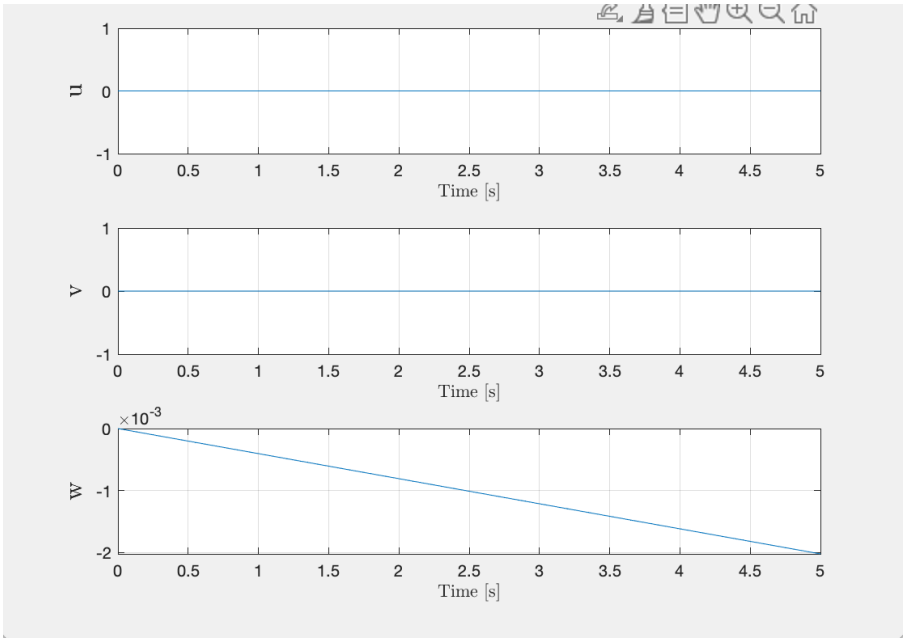

Figure 44. Body-fixed Linear Velocity [m/s].

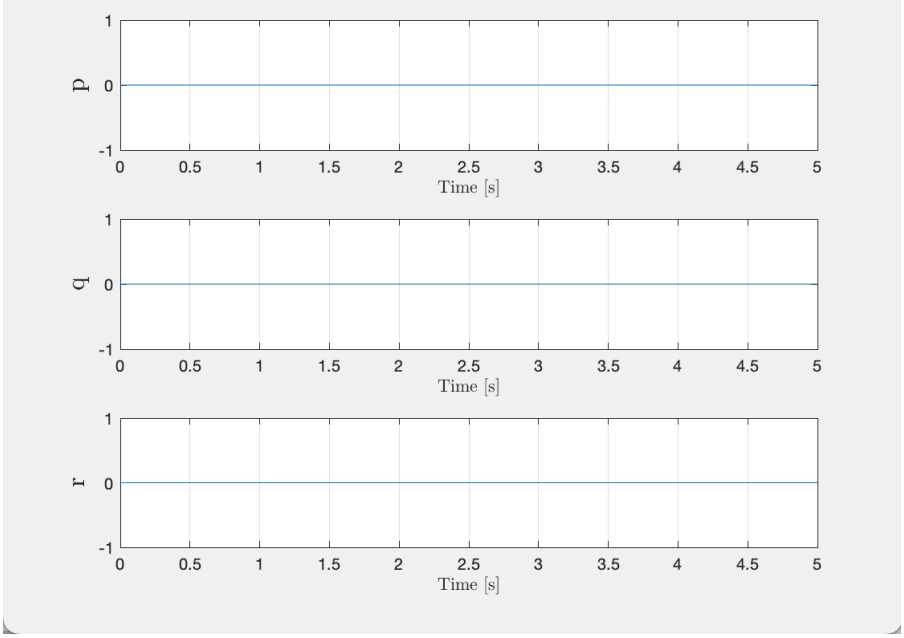

Figure 45. Body-fixed Angular Velocity [radians/s].

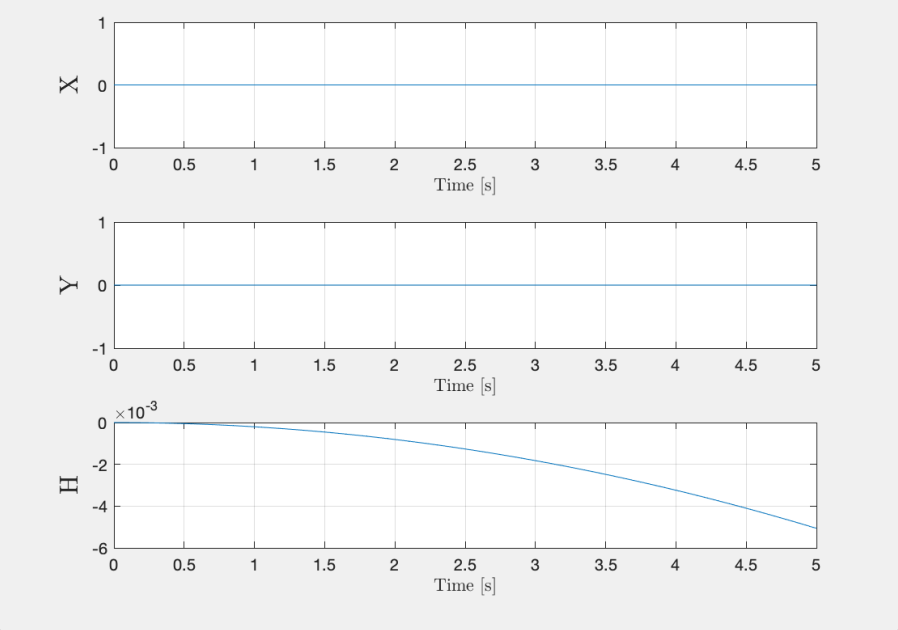

Figure 46. Inertial Position [m].

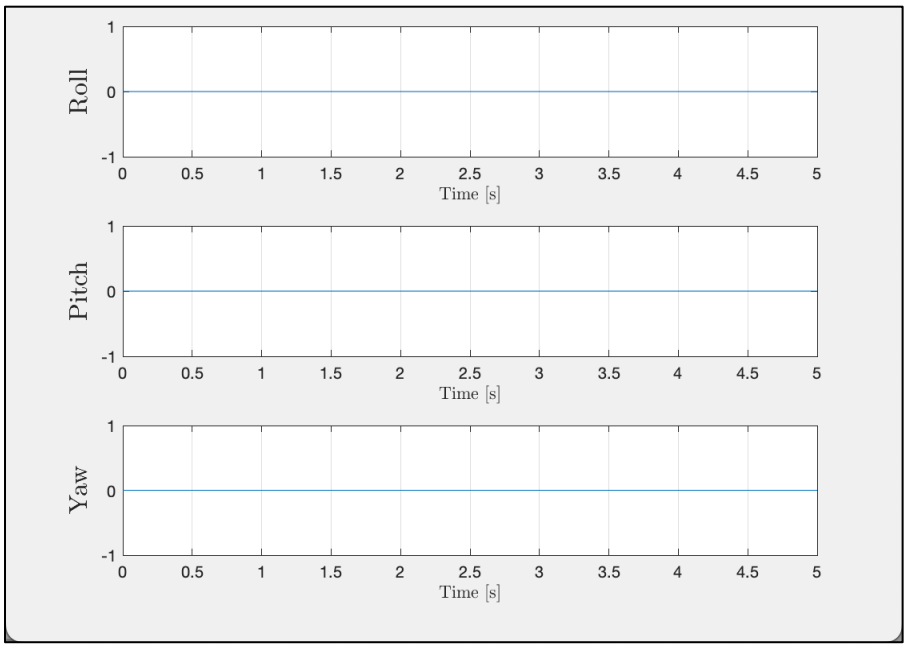

Figure 47. Euler Angles [radians].

Table 3. AUV Roll Maneuver Motor Data for a Mass of 2.72 kg (0.45 kg of payload).

Roll			
Motor	**RPM**	**Thrust [N]**	**Torque [N-m]**
1	8909	7.7874	0.1123
2	9065	8.0632	0.1163
3	9065	8.0632	0.1163
4	8909	7.7874	0.1123

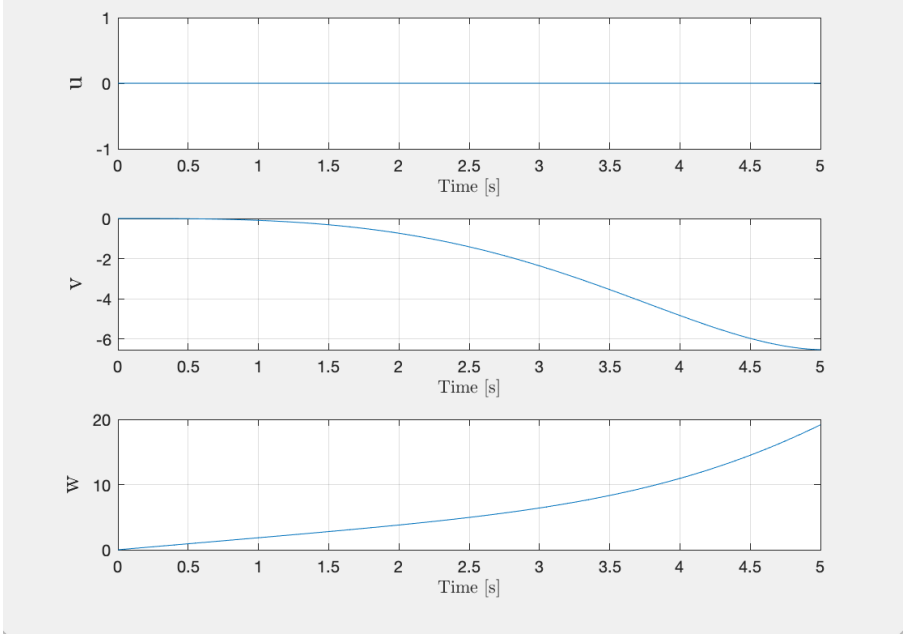

Figure 48. Body-fixed Linear Velocity [m/s].

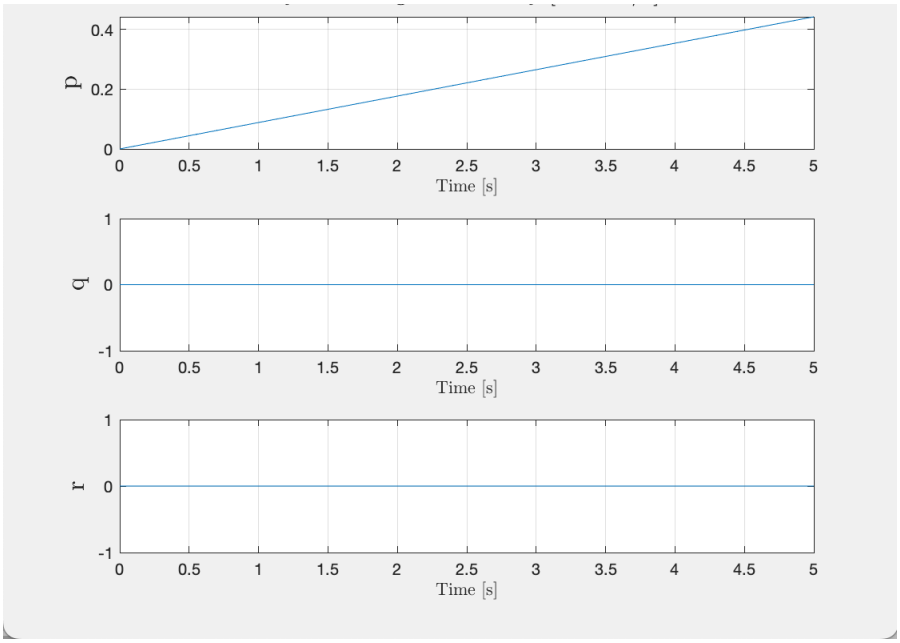

Figure 49. Body-fixed Angular Velocity [radians/s].

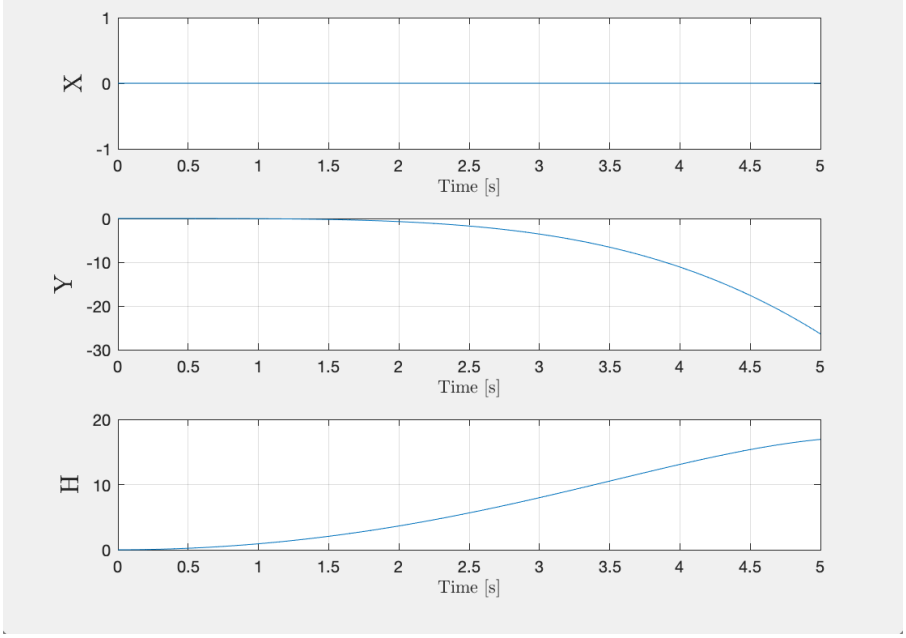

Figure 50. Inertial Position [m].

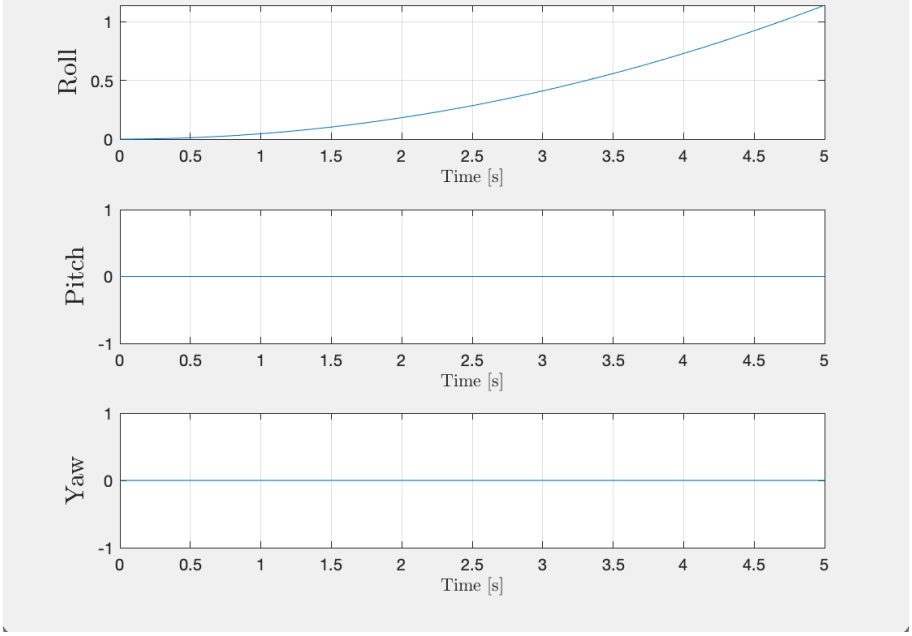

Figure 51. Euler Angles [radians].

Table 4. AUV Pitch Maneuver Motor Data for a Mass of 2.72 kg (0.45 kg of payload).

Pitch			
Motor	**RPM**	**Thrust [N]**	**Torque [N-m]**
1	8909	7.7874	0.1123
2	9065	8.0632	0.1163
3	8909	7.7874	0.1123
4	9065	8.0632	0.1163

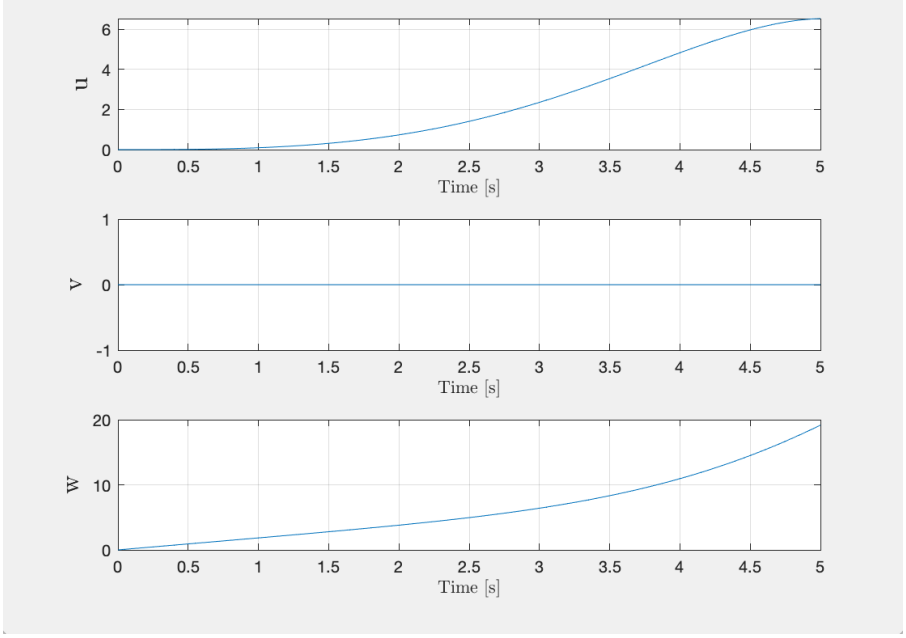

Figure 52. Body-fixed Linear Velocity [m/s].

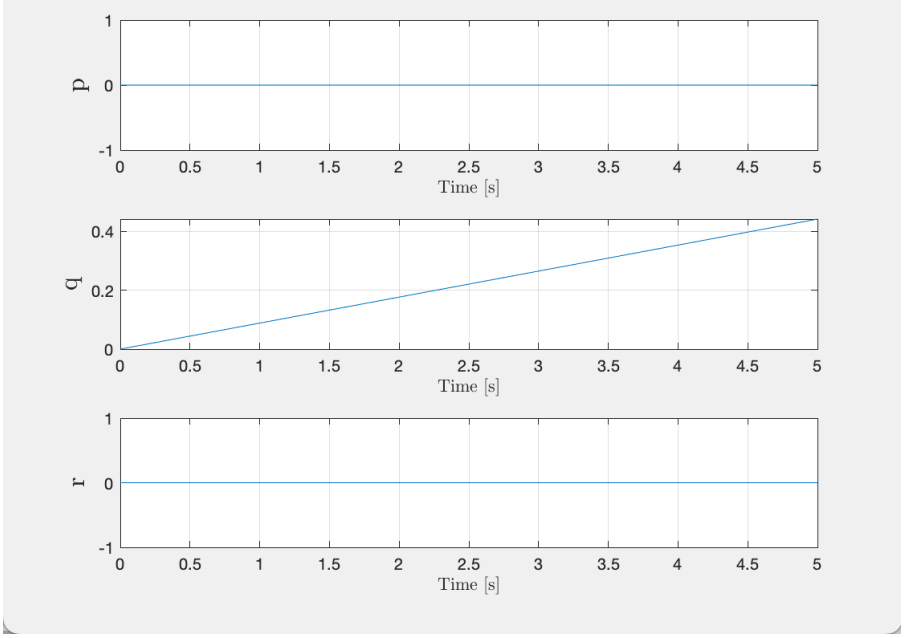

Figure 53. Body-fixed Angular Velocity [radians/s].

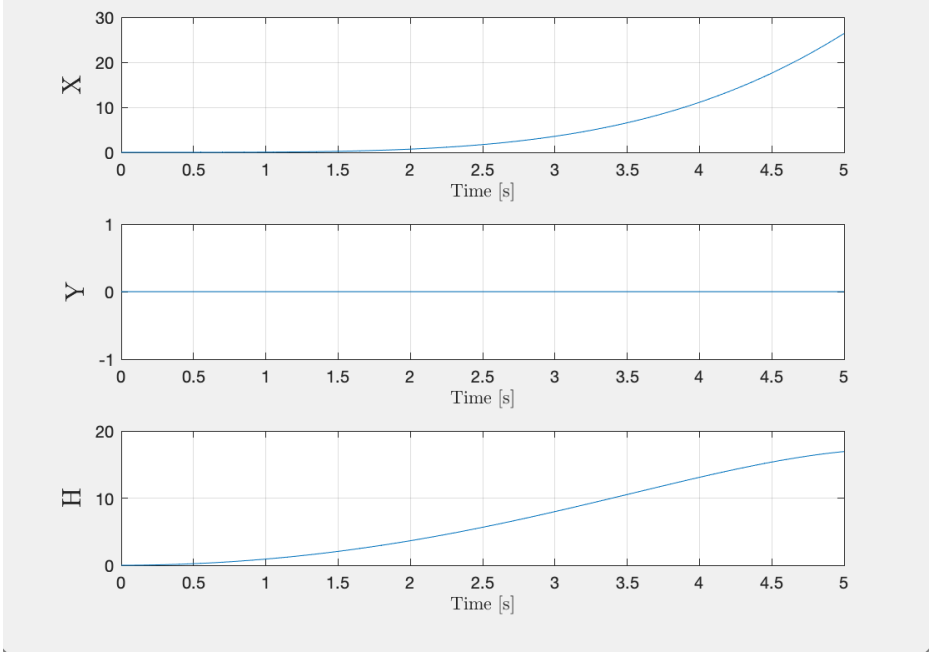

Figure 54. Inertial Position [m].

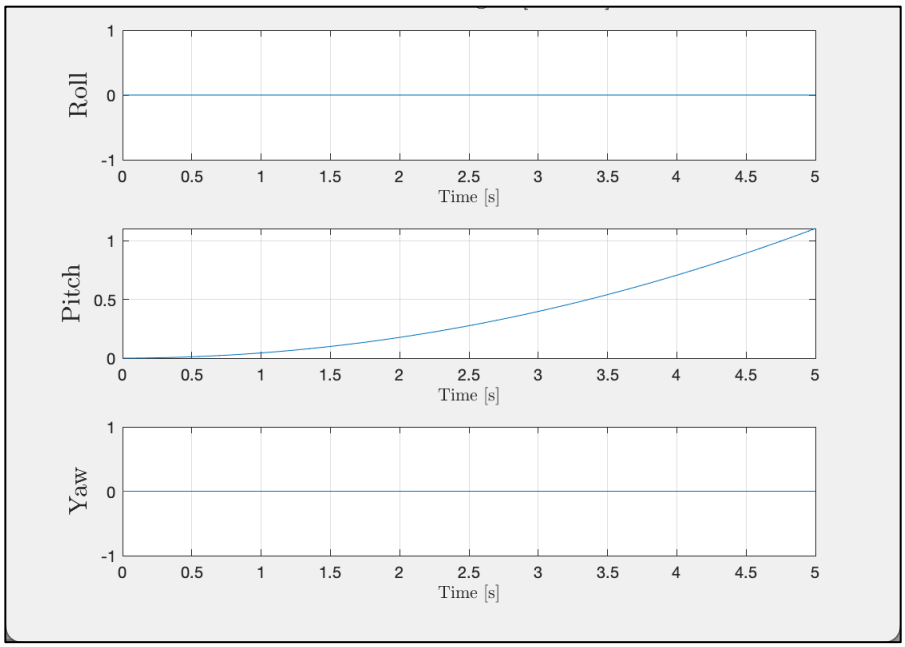

Figure 55. Euler Angles [radians].

Table 5. AUV Yaw Maneuver Motor Data for a Mass of 2.72 kg (0.45 kg of payload).

Yaw			
Motor	**RPM**	**Thrust [N]**	**Torque [N-m]**
1	8936	7.8348	0.1130
2	8936	7.8348	0.1130
3	7500	7.8348	0.0795
4	7500	7.8348	0.0795

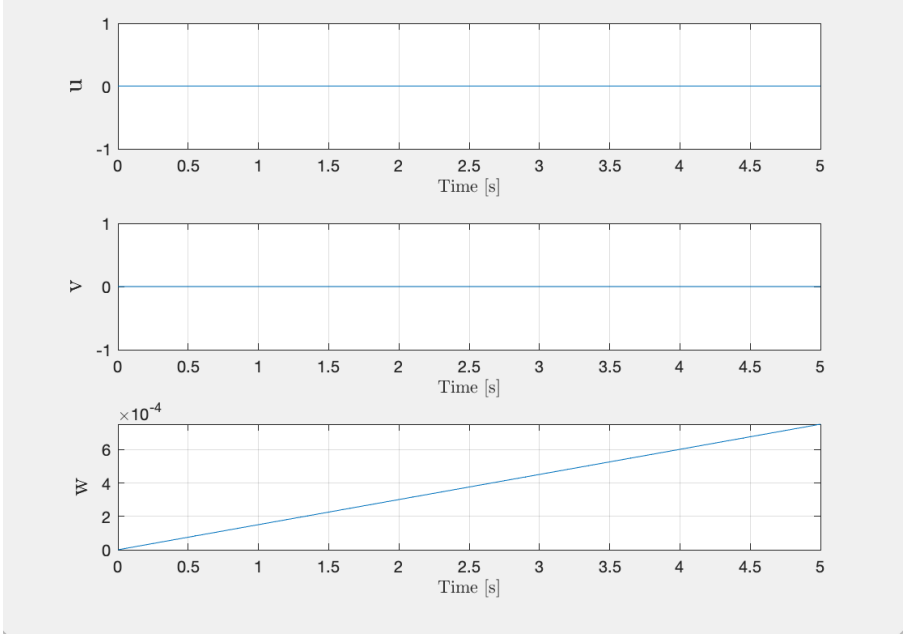

Figure 56. Body-fixed Linear Velocity [m/s].

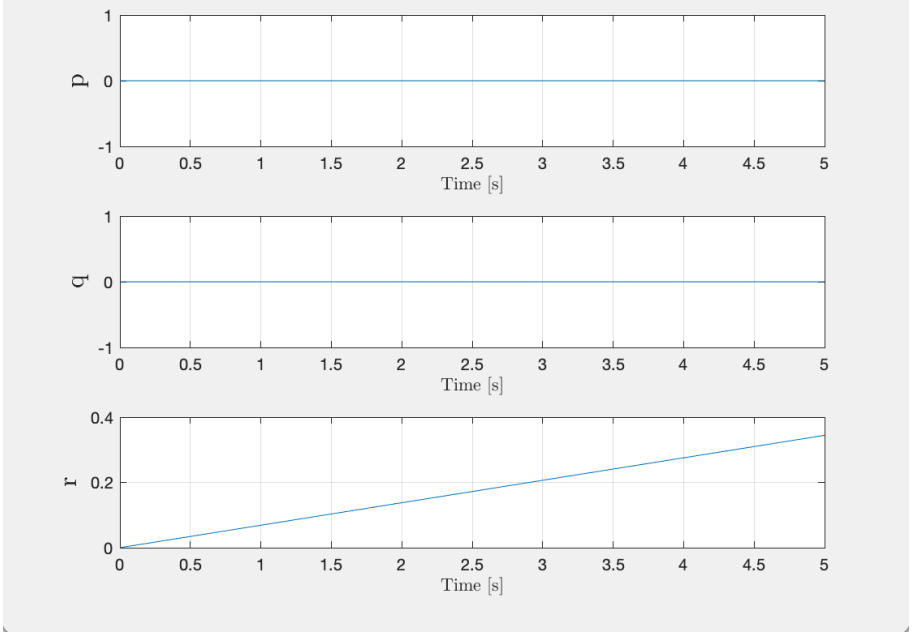

Figure 57. Body-fixed Angular Velocity [radians/s].

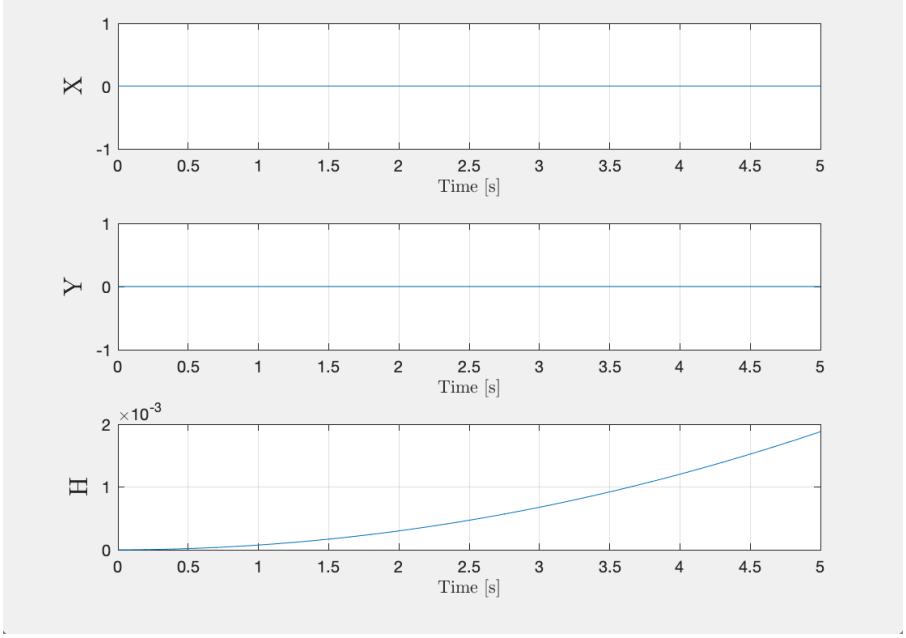

Figure 58. Inertial Position [m].

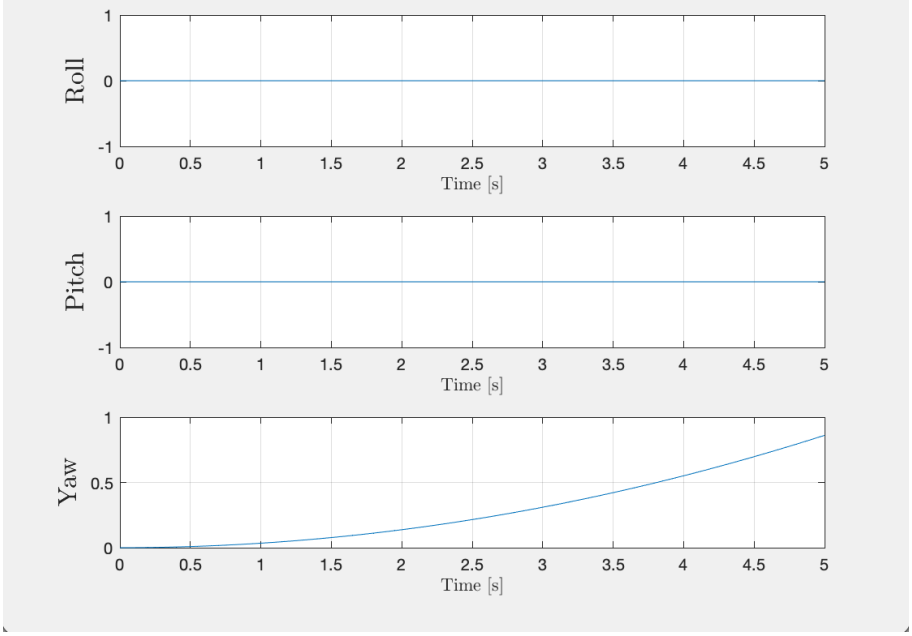

Figure 59. Euler Angles [radians].

Appendix C - Underwater Dynamics Derivation

Physical Model Simplifying Assumptions

1. AUV is treated as a rigid body.
2. The motors and propellers provide perfect thrust and control.
3. External disturbances are ignored.
4. AUV is neutrally buoyant when fully submerged.

Definitions

Linear Velocities in AUV Body-fixed Frame

$$\boldsymbol{v}^b = \begin{bmatrix} u \\ v \\ w \end{bmatrix}^b = \begin{bmatrix} \text{longitudinal velocity} \\ \text{lateral velocity} \\ \text{vertical velocity} \end{bmatrix}$$

Angular Velocities in AUV Body-fixed Frame

$$\boldsymbol{\omega} = \begin{bmatrix} p \\ q \\ r \end{bmatrix} = \begin{bmatrix} \text{roll rate} \\ \text{pitch rate} \\ \text{yaw rate} \end{bmatrix}$$

Forces acting on AUV

$$\boldsymbol{F} = \begin{bmatrix} F_x \\ F_y \\ F_z \end{bmatrix} = \begin{bmatrix} \text{force in X direction} \\ \text{force in Y direction} \\ \text{force in Z direction} \end{bmatrix}$$

$$F_D = \text{drag force of the water acting in the} - \text{x direction}$$

$$C_D = \text{drag coefficient of AUV}$$

$$A = \text{surface area perpendicular to water flow}$$

Moments acting on AUV

$$\boldsymbol{M} = \begin{bmatrix} L \\ M \\ N \end{bmatrix} = \begin{bmatrix} \text{moment about body} - \text{fixed x axis} \\ \text{moment about body} - \text{fixed y axis} \\ \text{moment about body} - \text{fixed z axis} \end{bmatrix}$$

Euler Angles

$$\boldsymbol{\Phi} = \begin{bmatrix} \phi \\ \theta \\ \psi \end{bmatrix} = \begin{bmatrix} \text{roll angle} \\ \text{pitch angle} \\ \text{yaw angle} \end{bmatrix}$$

Absolute Position in Inertial Navigation Frame

$$\boldsymbol{S} = \begin{bmatrix} X \\ Y \\ D \end{bmatrix} = \begin{bmatrix} \text{longitudinal position} \\ \text{lateral position} \\ \text{depth} \end{bmatrix}$$

Translational Motion

Newton's Second Law

$$\boldsymbol{F} = \frac{d\boldsymbol{p}}{dt} = m\frac{d\boldsymbol{v}}{dt} = m\boldsymbol{a}$$

Velocity in Body-fixed Frame

$$\boldsymbol{v}^b = \begin{bmatrix} u \\ v \\ w \end{bmatrix}^b = u\hat{x}_b + v\hat{y}_b + w\hat{z}_b$$

Acceleration in Body-fixed Frame

$$\left(\frac{d\boldsymbol{v}^b}{dt}\right)_{inertial} = \left(\frac{du}{dt}\hat{x}_b + \frac{dv}{dt}\hat{y}_b + \frac{dw}{dt}\hat{z}_b\right) + \left(u\frac{d\hat{x}_b}{dt} + v\frac{d\hat{y}_b}{dt} + w\frac{d\hat{z}_b}{dt}\right)$$

$$\dot{\boldsymbol{v}}_n^b = \dot{\boldsymbol{v}}^b + \dot{\boldsymbol{\omega}}_n^b \times \boldsymbol{v}^b$$

$$\dot{\boldsymbol{v}}_n^b = \begin{bmatrix} \dot{u} \\ \dot{v} \\ \dot{w} \end{bmatrix} + \begin{bmatrix} 0 & -r & q \\ r & 0 & -p \\ -q & p & 0 \end{bmatrix} \begin{bmatrix} u \\ v \\ w \end{bmatrix} = \begin{bmatrix} \dot{u} + qw - rv \\ \dot{v} + ru - pw \\ \dot{w} + pv - qu \end{bmatrix}$$

Force Exerted by Propeller Thrust

$$F_D = \frac{1}{2}\left(\frac{C_D A}{m}\right)\rho u^2$$

$$\boldsymbol{F}_{prop} = \begin{bmatrix} F_x \\ F_y \\ F_z \end{bmatrix} = \begin{bmatrix} F_1 + F_3 - F_D \\ 0 \\ 0 \end{bmatrix}$$

Gravitational Force in Inertial and Body-fixed Frame

Based on our assumption that our AUV is neutrally buoyant, the buoyancy force cancels out the gravitational force acting on the AUV.

$$\boldsymbol{F}_{grav}^n = \boldsymbol{F}_{grav}^b = \begin{bmatrix} 0 \\ 0 \\ 0 \end{bmatrix}$$

$$\boldsymbol{F}_{prop} + \boldsymbol{F}_{grav} = m\dot{\boldsymbol{v}}_n^b$$

$$\begin{bmatrix} F_1 + F_3 - F_D \\ 0 \\ 0 \end{bmatrix} = m \begin{bmatrix} \dot{u} + qw - rv \\ \dot{v} + ru - pw \\ \dot{w} + pv - qu \end{bmatrix}$$

Equations of Motion (Linear Acceleration)

$$\dot{u} = \frac{(F_1 + F_3 - F_D)}{m} - qw + rv$$

$$\dot{v} = -ru + pw$$

$$\dot{w} = -pv + qu$$

Rotational Motion

Moment Angular Velocity Relationship

$$M = \frac{d\boldsymbol{H}}{dt} = I\frac{d\boldsymbol{\omega}}{dt} = I\boldsymbol{\Omega}$$

Chain Rule Derivation

$$\boldsymbol{M} = I\frac{d\boldsymbol{\omega}}{dt} \rightarrow \boldsymbol{M} = I\dot{\boldsymbol{\omega}}_n^b + \boldsymbol{\omega}_n^b \times I\boldsymbol{\omega}_n^b$$

Moment of Inertia Matrix

$$I = \begin{bmatrix} I_{xx} & -I_{xy} & -I_{xz} \\ -I_{xy} & I_{yy} & -I_{yz} \\ -I_{xz} & -I_{yz} & I_{zz} \end{bmatrix}$$

$$\boldsymbol{M} = I\dot{\boldsymbol{\omega}}_n^b + \boldsymbol{\omega}_n^b \times I\boldsymbol{\omega}_n^b$$

$$\begin{bmatrix} L \\ M \\ N \end{bmatrix} = \begin{bmatrix} I_{xx} & -I_{xy} & -I_{xz} \\ -I_{xy} & I_{yy} & -I_{yz} \\ -I_{xz} & -I_{yz} & I_{zz} \end{bmatrix}\begin{bmatrix} \dot{p} \\ \dot{q} \\ \dot{r} \end{bmatrix} + \begin{bmatrix} 0 & -r & q \\ r & 0 & -p \\ -q & p & 0 \end{bmatrix}\begin{bmatrix} I_{xx} & -I_{xy} & -I_{xz} \\ -I_{xy} & I_{yy} & -I_{yz} \\ -I_{xz} & -I_{yz} & I_{zz} \end{bmatrix}\begin{bmatrix} p \\ q \\ r \end{bmatrix}$$

$$\begin{bmatrix} L \\ M \\ N \end{bmatrix} = \begin{bmatrix} I_{xx}\dot{p} - I_{xy}\dot{q} - I_{xz}\dot{r} - p\left(I_{xz}q - I_{xy}r\right) - q\left(I_{yz}q + I_{yy}r\right) + r\left(I_{zz}q + I_{yz}r\right) \\ I_{yy}\dot{q} - I_{xy}\dot{p} - I_{yz}\dot{r} + p(I_{xz}p + I_{xx}r) + q\left(I_{yz}p - I_{xy}r\right) - r(I_{zz}p + I_{xz}r) \\ I_{zz}\dot{r} - I_{yz}\dot{q} - I_{xz}\dot{p} - p\left(I_{xy}q + I_{xx}q\right) + q\left(I_{yy}p + I_{xy}q\right) - r\left(I_{yz}p - I_{xz}q\right) \end{bmatrix}$$

From our one-to-one SolidWorks model, the computed moment of inertia matrix came out to:

$$I = \begin{bmatrix} 0.014002 & -0.001114 & -0.001352 \\ -0.001114 & 0.029709 & 0.000313 \\ -0.001352 & 0.000313 & 0.041018 \end{bmatrix} kg * m^2$$

Since the off-diagonal elements of the moment of inertia matrix are two to even three orders of magnitude smaller than the diagonal elements we went with the assumption of our moment of inertia matrix being:

$$I = \begin{bmatrix} Ixx & 0 & 0 \\ 0 & Iyy & 0 \\ 0 & 0 & Izz \end{bmatrix}$$

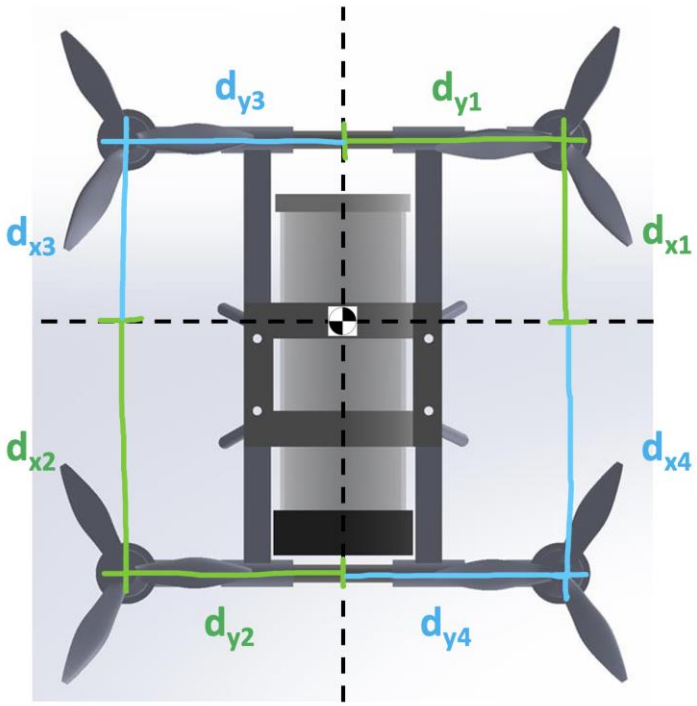

Figure 60: X and Y displacement from Body-fixed Origin (AUV CoM).

$$L = T_1 - T_3$$

$$M = (F_1 + F_2)d_{2x}$$

$$N = T_2 - T_4$$

Equations of Motion (Angular Acceleration)

$$\dot{p} = \frac{\left(L + I_{xy}\dot{q} + I_{xz}\dot{r} + p\left(I_{xz}q - I_{xy}r\right) + q\left(I_{yz}q + I_{yy}r\right) - r\left(I_{zz}q + I_{yz}r\right)\right)}{I_{xx}}$$

$$\dot{q} = \frac{\left(M + I_{xy}\dot{p} + I_{yz}\dot{r} - p(I_{xz}p + I_{xx}r) - q\left(I_{yz}p - I_{xy}r\right) + r(I_{zz}p + I_{xz}r)\right)}{I_{yy}}$$

$$\dot{r} = \frac{\left(N + I_{xz}\dot{p} + I_{yz}\dot{q} + p\left(I_{xy}p + I_{xx}q\right) - q\left(I_{yy}p + I_{xy}q\right) + r\left(I_{yz}p - I_{xz}q\right)\right)}{I_{zz}}$$

However, with the assumption of our moment of inertia matrix being:

$$I = \begin{bmatrix} Ixx & 0 & 0 \\ 0 & Iyy & 0 \\ 0 & 0 & Izz \end{bmatrix}$$

The angular acceleration equations simplify to:

$$\dot{p} = \frac{L}{I_{xx}} - \left(\frac{I_{yy} - I_{zz}}{I_{xx}}\right) q\, r$$

$$\dot{q} = \frac{M}{I_{yy}} - \left(\frac{I_{zz} - I_{xx}}{I_{yy}}\right) p\, r$$

$$\dot{r} = \frac{N}{I_{zz}} - \left(\frac{I_{xx} - I_{yy}}{I_{zz}}\right) p\, q$$

Just as the transition from the body-fixed to the inertial navigation frame was employed in formulating the three translational and three rotational equations of motion for aerial dynamics, a similar approach was adopted for deriving underwater dynamics using rotation matrices. This methodology entails the establishment of two intermediary frames: R1, formed by a yaw rotation of the inertial navigation frame, and R2, generated through a subsequent pitch rotation of R1. Finally, R3 is obtained by applying a roll rotation to R2, resulting in the establishment of the body-fixed reference frame. These intermediary frames play a crucial role in deriving equations of motion for the AUV. They are pivotal for a seamless transition from the inertial navigation frame to the body-fixed reference frame, facilitating accurate modeling and analysis of the AUV's dynamics and behavior.

Equations of Motion in Inertial Navigation Frame

Linear Velocity Rotation Matrix (Body-fixed to Inertial Reference Frame)

$$R_b^n = \begin{bmatrix} \mathrm{c}(\theta)\,\mathrm{c}(\phi) & \mathrm{s}(\phi)\,\mathrm{s}(\theta)\,\mathrm{c}(\psi) - \mathrm{c}(\phi)\,\mathrm{s}(\psi) & \mathrm{s}(\phi)\,\mathrm{s}(\psi) + \mathrm{c}(\phi)\mathrm{s}(\theta)\mathrm{c}(\psi) \\ \mathrm{c}(\theta)\mathrm{s}(\psi) & \mathrm{c}(\phi)\,\mathrm{c}(\psi) + \mathrm{s}(\phi)\,\mathrm{s}(\theta)\,\mathrm{s}(\psi) & \mathrm{c}(\phi)\,\mathrm{s}(\theta)\,\mathrm{s}(\psi) - \mathrm{s}(\phi)\,\mathrm{c}(\psi) \\ -\mathrm{s}(\theta) & \mathrm{s}(\phi)\,\mathrm{c}(\theta) & \mathrm{c}(\phi)\,\mathrm{c}(\theta) \end{bmatrix}$$

Linear Velocity

$$\dot{X} = (\mathrm{c}(\theta)\,\mathrm{c}(\phi))u + (-\mathrm{c}(\phi)\,\mathrm{s}(\psi) + \mathrm{s}(\phi)\,\mathrm{s}(\theta)\,\mathrm{c}(\psi))v + (\mathrm{s}(\phi)\,\mathrm{s}(\psi) + \mathrm{c}(\phi)\,\mathrm{s}(\theta)\,\mathrm{c}(\psi))w$$

$$\dot{Y} = (\mathrm{c}(\theta)\,\mathrm{s}(\psi))u + (\mathrm{c}(\phi)\,\mathrm{c}(\psi) + \mathrm{s}(\phi)\,\mathrm{s}(\theta)\,\mathrm{s}(\psi))v + (-\mathrm{s}(\phi)\,\mathrm{c}(\psi) + \mathrm{c}(\phi)\,\mathrm{s}(\theta)\,\mathrm{s}(\psi))w$$

$$\dot{H} = (-\mathrm{s}(\theta))u + (\mathrm{s}(\phi)\,\mathrm{c}(\theta))v + (\mathrm{c}(\phi)\,\mathrm{c}(\theta))w$$

Angular Velocity Rotation Matrix (Body-fixed to Inertial Reference Frame)

$$R_b^n = \begin{bmatrix} 1 & \sin(\phi)\tan(\theta) & \cos(\phi)\tan(\theta) \\ 0 & \cos(\phi) & -\sin(\phi) \\ 0 & \sin(\phi)\sec(\theta) & \cos(\phi)\sec(\theta) \end{bmatrix}$$

Euler Angles Rate of Change

$$\dot{\phi} = p + q(\sin(\phi)\tan(\theta)) + r(\cos(\phi)\tan(\theta))$$

$$\dot{\theta} = q(\cos(\phi)) - r(\sin(\phi))$$

$$\dot{\psi} = q(\sin(\phi)\sec(\theta)) + r(\cos(\phi)\sec(\theta))$$

Rotation matrices play a fundamental role in deriving equations of motion, serving as indispensable tools in the analysis of dynamic systems. These matrices are crucial for representing the orientation and transformation of coordinate systems, enabling a seamless transition between different frames of reference. In the context of dynamics, rotation matrices are particularly vital when dealing with complex motions such as those encountered in aerial and underwater vehicles. They provide a systematic and mathematically rigorous way to express the relationship between inertial and body-fixed frames. By establishing intermediary frames through successive rotations, as exemplified in the yaw, pitch, and roll rotations, rotation matrices facilitate the derivation of equations of motion for these systems. This structured approach not only ensures accuracy in modeling but also allows for a comprehensive understanding of the intricate dynamics governing the behavior of objects in motion, making rotation matrices an essential component in the realm of dynamic systems analysis.

Appendix D - Underwater Dynamics Validation Results

Table 6: AUV Propel Forward (Constant Pitch) Maneuver Motor Data for a Mass of 2.72 kg (0.45 kg of payload).

Propel Forward			
Motor	**RPM**	**Thrust [N]**	**Torque [N-m]**
1	100	0.9007	0.0116
2	28.18	0	0
3	**100**	0.9007	0.0116
4	28.18	0	0

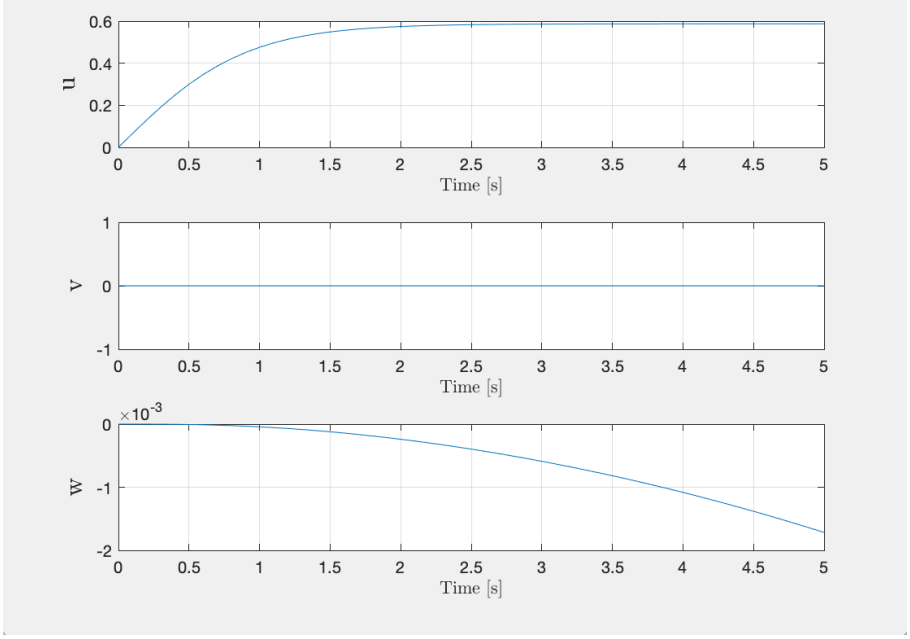

Figure 61. Body-fixed Linear Velocity [m/s].

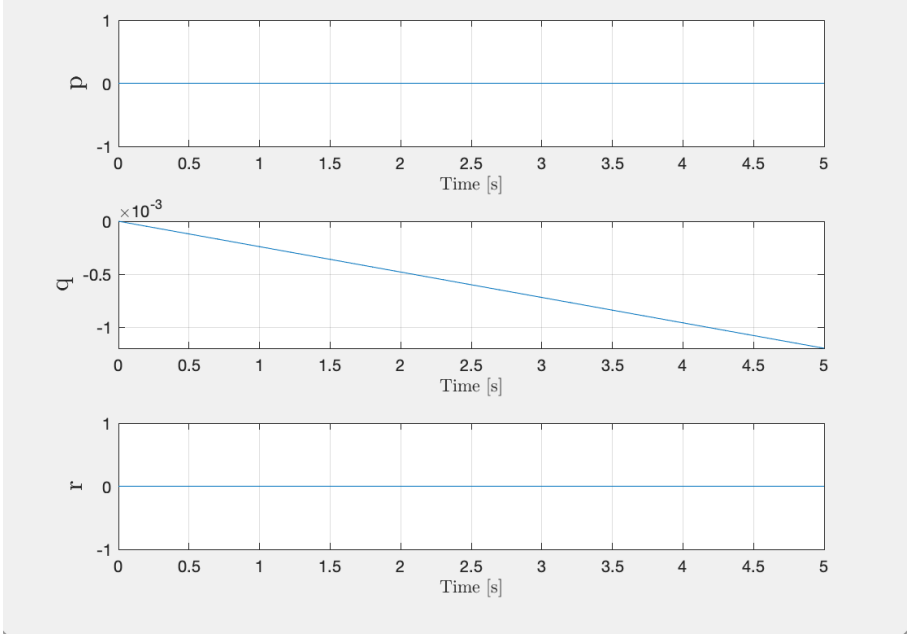

Figure 62. Body-fixed Angular Velocity [radians/s].

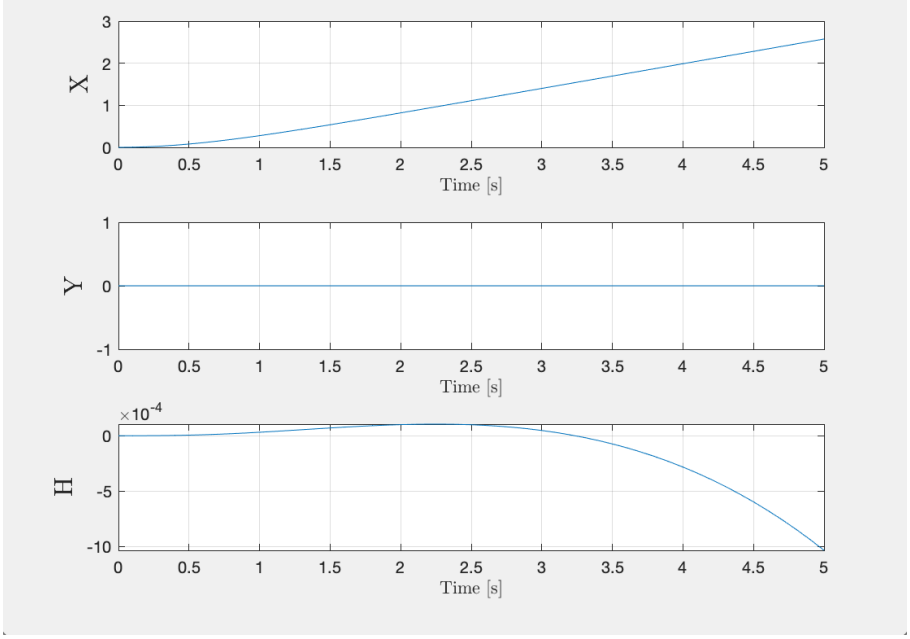

Figure 63. Inertial Position [m].

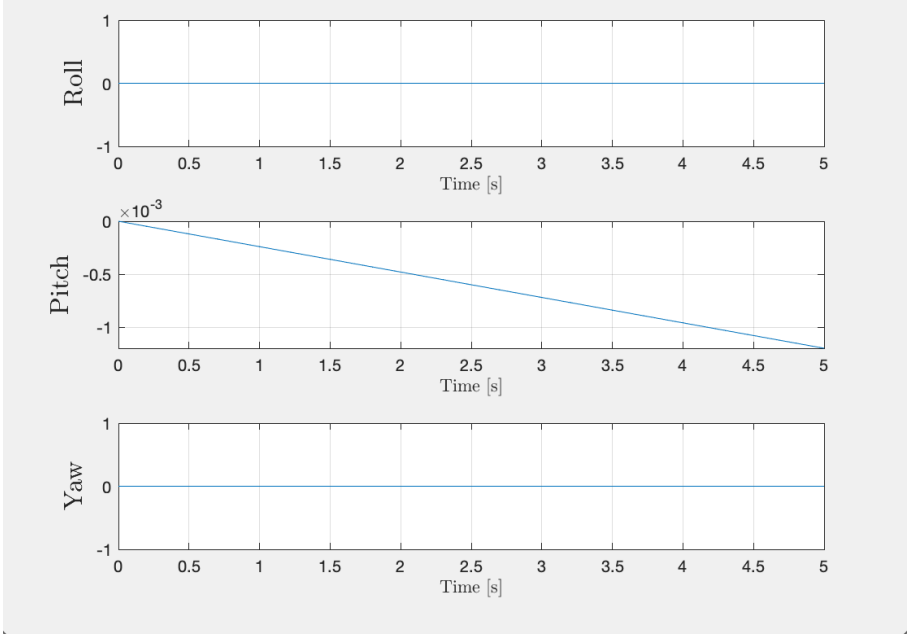

Figure 64. Euler Angles [radians].

Table 7: AUV Pitch Maneuver Motor Data for a Mass of 2.72 kg (0.45 kg of payload).

Pitch			
Motor	**RPM**	**Thrust [N]**	**Torque [N-m]**
1	100	0.9007	0.0116
2	30.1	0.0142	0
3	100	0.9007	0.0116
4	30.1	0.0142	0

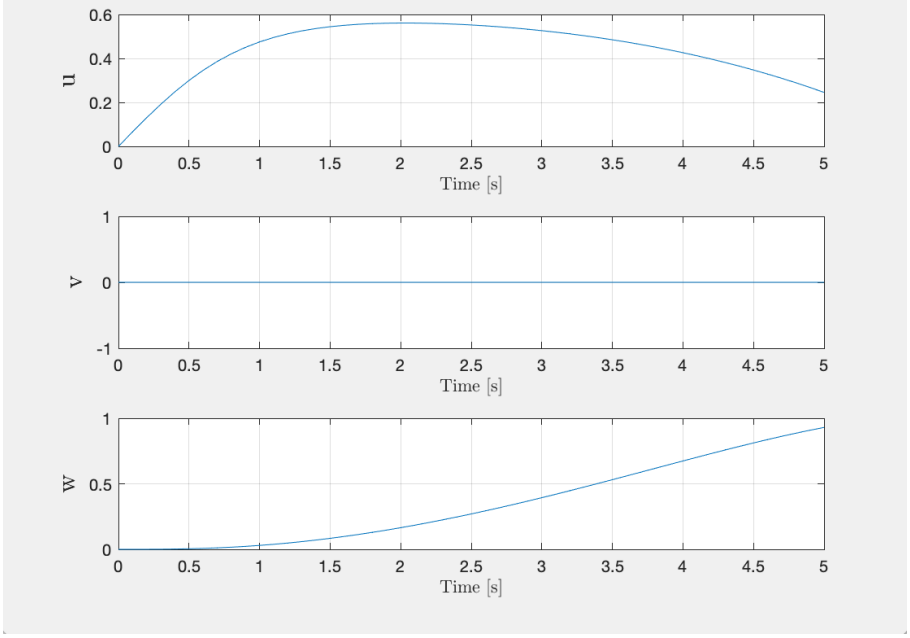

Figure 65. Body-fixed Linear Velocity [m/s].

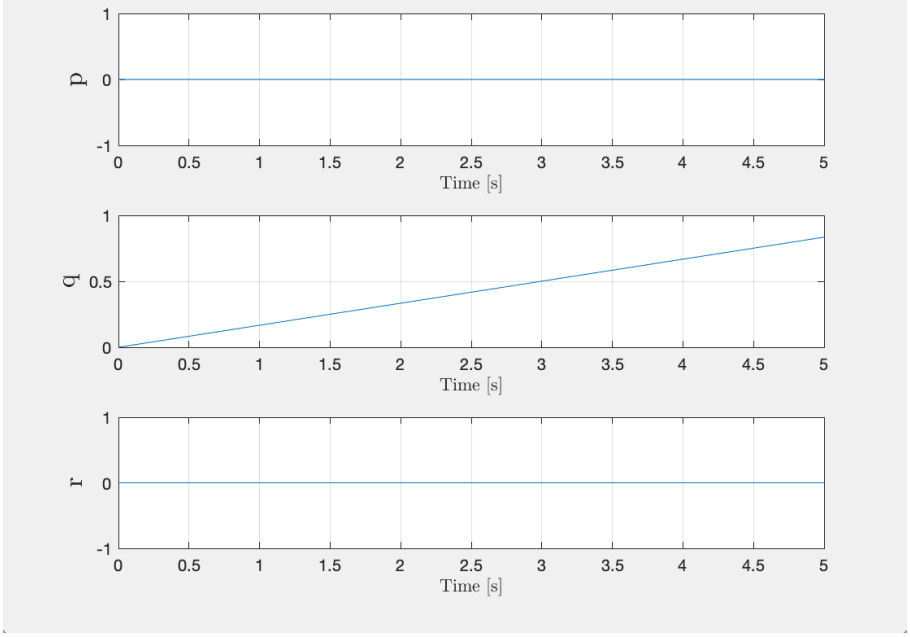

Figure 66. Body-fixed Angular Velocity [radians/s].

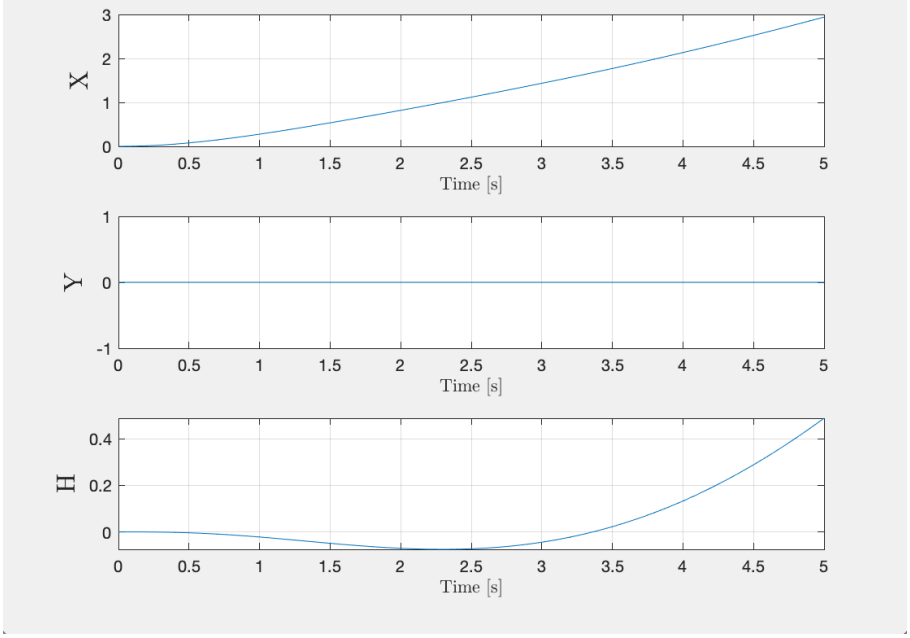

Figure 67. Inertial Position [m].

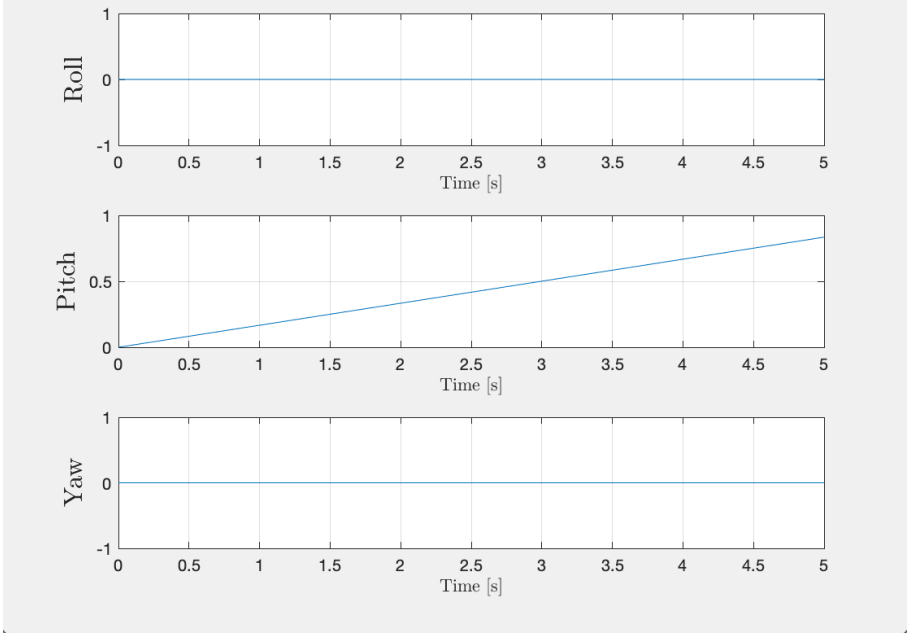

Figure 68. Euler Angles [radians].

Table 8: AUV Roll Maneuver Motor Data for a mass of 2.72 kg (0.45 kg of payload).

Roll			
Motor	**RPM**	**Thrust [N]**	**Torque [N-m]**
1	100	0.9007	0.0116
2	30	0.0134	0
3	93	7.7874	0.0100
4	30	0.0134	0

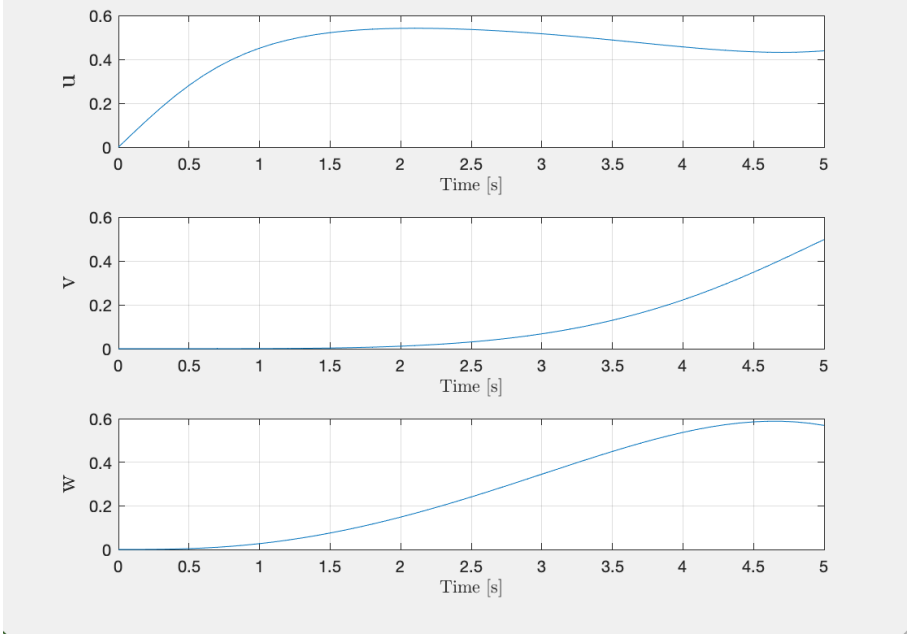

Figure 69. Body-fixed Linear Velocity [m/s].

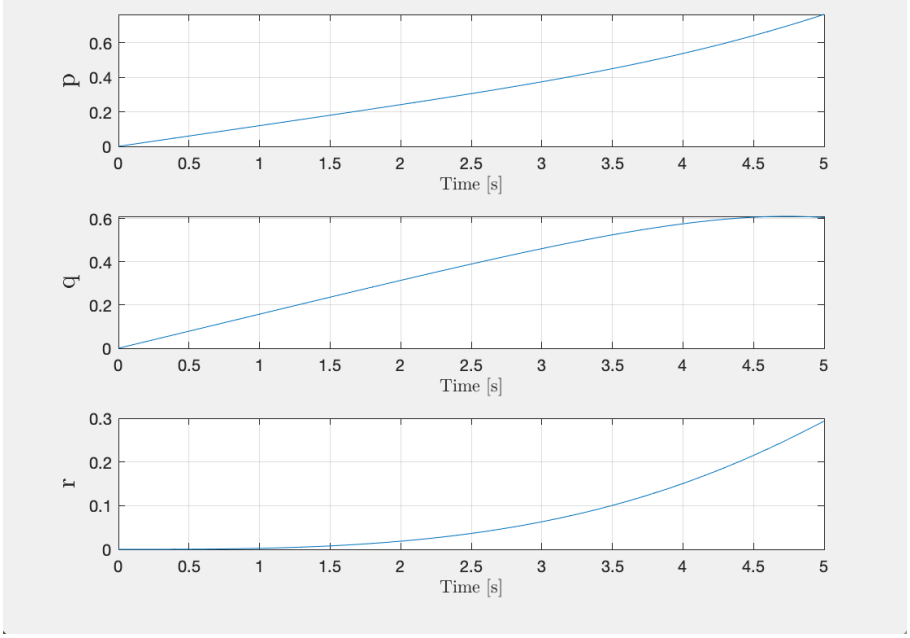

Figure 70. Body-fixed Angular Velocity [radians/s].

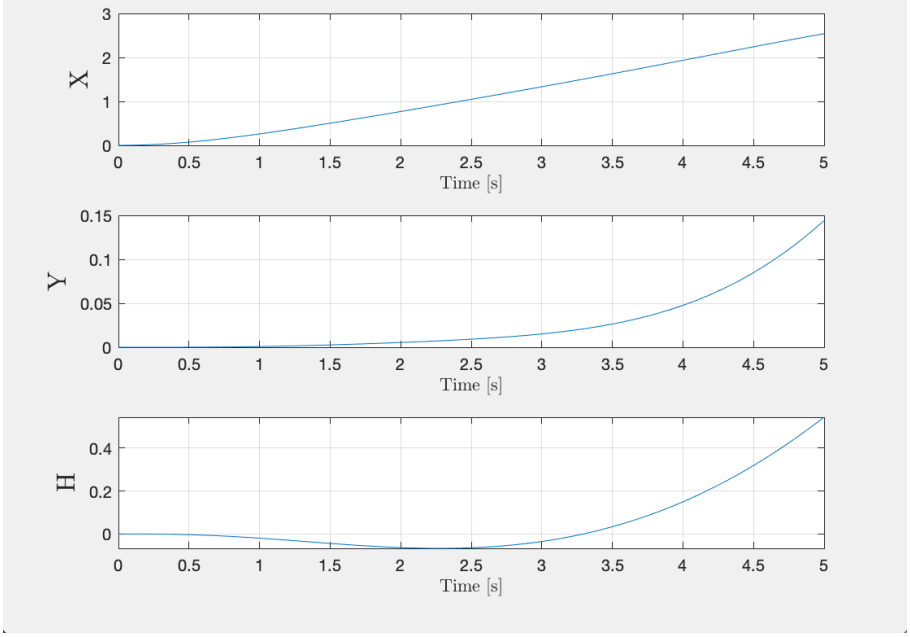

Figure 71. Inertial Position [m].

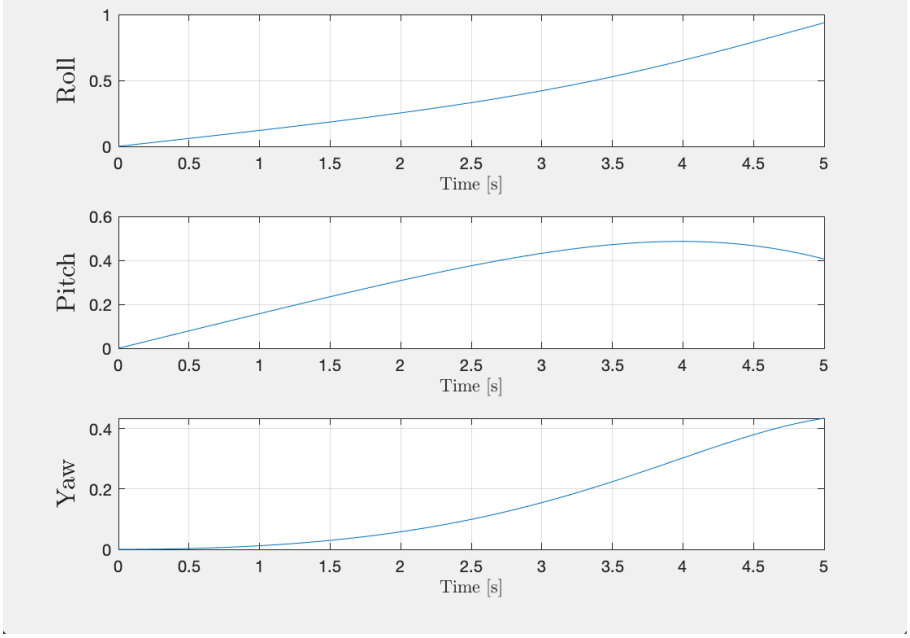

Figure 72. Euler Angles [radians].